



# The influence of oxygen isotope exchange between CO<sub>2</sub> and H<sub>2</sub>O in natural CO<sub>2</sub>-rich spring waters: Implications for geothermometry



Rūta Karolytė<sup>\*</sup>, Sascha Serno<sup>1</sup>, Gareth Johnson, Stuart M.V. Gilfillan

School of GeoSciences, University of Edinburgh, Grant Institute, James Hutton Road, Edinburgh, EH9 3FE, United Kingdom

## ARTICLE INFO

### Article history:

Received 10 January 2017

Received in revised form

17 May 2017

Accepted 22 June 2017

Available online 27 June 2017

Editorial handling by Prof. M. Kersten.

### Keywords:

Oxygen isotopes

CO<sub>2</sub> springs

Mineral springs

Geothermometry

Geochemical modelling

Water-rock reactions

Low temperature aqueous systems

## ABSTRACT

Oxygen isotope ratio ( $\delta^{18}\text{O}$ ) value deviations from the Meteoric Water Line with no significant change in the hydrogen isotope ( $\delta^2\text{H}$ ) composition have been reported in naturally occurring CO<sub>2</sub>-rich waters from around the world. Here we review the effects of oxygen isotope exchange with CO<sub>2</sub>, high temperature equilibration with bedrock minerals and mineral dissolution and precipitation reactions on the CO<sub>2</sub>-rich water isotopic composition. We present two case studies from Daylesford (Australia) and Pah Tempe (Utah, USA) mineral springs, where we use a numerical geochemical modelling approach to resolve the influence of low temperature water-rock interactions and CO<sub>2</sub> equilibration to the oxygen isotope ranges observed in the mineral waters. In both cases, we find that mineral dissolution – precipitation reactions are unlikely to have a significant effect on the groundwater isotopic compositions, and that the observed  $\delta^{18}\text{O}$  values in natural CO<sub>2</sub> springs can be simply explained by equilibrium fractionation between water and free phase CO<sub>2</sub>. Traditionally, the interaction of CO<sub>2</sub> and water in a natural CO<sub>2</sub>-rich groundwater setting has only been associated with water <sup>18</sup>O depletion and this is the first study to consider <sup>18</sup>O enrichment. We establish that in a natural setting, CO<sub>2</sub> and water equilibration can result in water <sup>18</sup>O depletion or enrichment, and that the change in the oxygen isotope composition ultimately depends on the initial CO<sub>2</sub> and water  $\delta^{18}\text{O}$  values. Our new conceptual model therefore provides a mechanism to explain water <sup>18</sup>O enrichment at ambient temperatures. This finding is critical for the use of  $\delta^{18}\text{O}$  in groundwater geothermometry and for the interpretation of natural water circulation depths: we argue that in some cases, natural waters previously interpreted as geothermal based on their oxygen isotope composition may actually have acquired their isotopic signature through interaction with CO<sub>2</sub> at ambient temperatures.

© 2017 The Authors. Published by Elsevier Ltd. This is an open access article under the CC BY license (<http://creativecommons.org/licenses/by/4.0/>).

## 1. Introduction

The stable isotope ratios in groundwater are useful indicators of a wide range of geological conditions associated with groundwater reservoirs and mineral springs. Applications include interpretation of water origin (Harris et al., 1997; Ziegler, 2006; Demlie and Titus, 2015), residence times (Vuataz and Goff, 1986; Hearn et al., 1989), migration pathways and mixing trends (Hearn et al., 1989; Siegel et al., 2004; Wilkinson et al., 2009; Delalande et al., 2011), temperature and circulation depths (Ziegler, 2006; Nelson et al., 2009), fault and fracture permeability to fluids (Cerón et al., 1998; Losh

et al., 1999; Lions et al., 2014), local rainfall variations (Burns and Matter, 1995) and paleoclimates (Hays and Grossman, 1991). These geological interpretations rely on the identification of fundamental natural processes controlling kinetic and equilibrium fractionation of water stable oxygen and hydrogen isotopes (Fig. 1). Here we investigate the effect of water interaction with CO<sub>2</sub> and its impact on the isotopic composition of natural waters. In particular, we investigate changes in the oxygen isotope ratio ( $\delta^{18}\text{O}$ ) values of water independent of changes in hydrogen isotope ratios ( $\delta^2\text{H}$ ).

The main processes that result in water <sup>18</sup>O depletion or enrichment without affecting hydrogen isotope ratios are oxygen isotope exchange with CO<sub>2</sub> and isotope exchange with bedrock minerals, either through low temperature mineral dissolution and precipitation, or diffusion at high temperatures (Fig. 1). Water <sup>18</sup>O enrichment relative to the Meteoric Water Line (MWL) with no change in the hydrogen isotope ratio has been traditionally associated with oxygen isotope exchange with bedrock minerals or

<sup>\*</sup> Corresponding author.

E-mail address: [ruta.karolyte@ed.ac.uk](mailto:ruta.karolyte@ed.ac.uk) (R. Karolytė).

<sup>1</sup> Present address: School of Mechanical and Aerospace Engineering, Queen's University, Ashby Building, 125 Stranmillis Road, Belfast, BT9 5AH, United Kingdom.

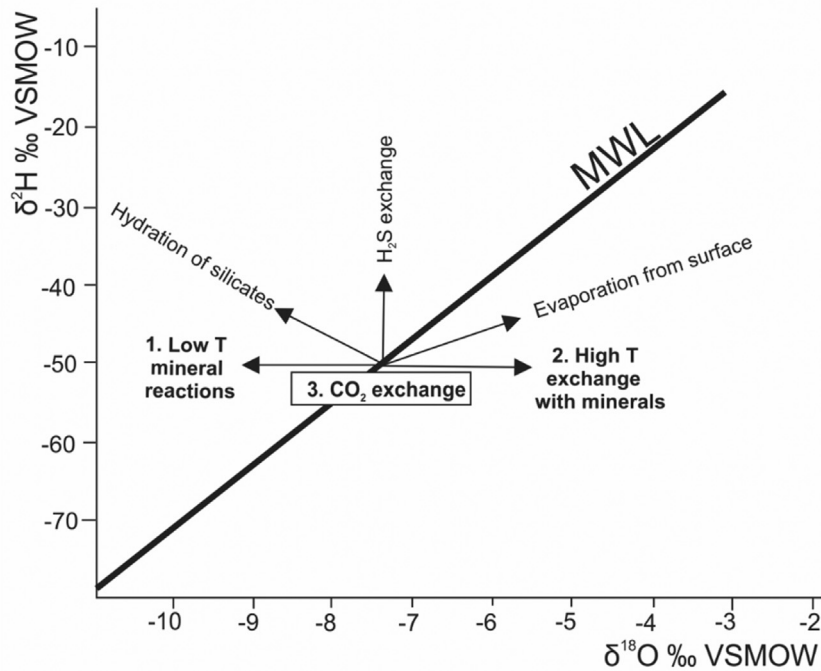


Fig. 1. Natural processes affecting water  $\delta^{18}\text{O}$  and  $\delta^2\text{H}$  values (adapted from D'Amore and Panichi, 1987).

water-steam separation in geothermal conditions (e.g. Clayton and Steiner, 1975; Matsuhisa et al., 1979; Giggenbach, 1992). Due to the lack of other reported water  $^{18}\text{O}$  enriching mechanisms it has become common practice to interpret  $^{18}\text{O}$  enrichment in water as evidence for geothermal conditions (e.g. Cerón et al., 1998; Nelson et al., 2009). In contrast, oxygen isotope exchange with  $\text{CO}_2$  has been associated with water  $^{18}\text{O}$  depletion (Clark and Fritz, 1997; D'Amore and Panichi, 1987). However, recent applications of oxygen isotopes to monitor injected  $\text{CO}_2$  in Carbon Capture and Storage (CCS) reservoirs have demonstrated that the water isotopic composition after  $\text{CO}_2$  injection is primarily dependent on the oxygen isotope ratios of pre-injection water and  $\text{CO}_2$  and of the degree of  $\text{CO}_2$  saturation in the water and gas phases in the reservoir pore space (Kharaka et al., 2006; Johnson et al., 2011; Johnson and Mayer, 2011; Serno et al., 2016). Applying this new knowledge to naturally occurring  $\text{CO}_2$ -rich mineral springs, we re-evaluate previous interpretations of  $\delta^{18}\text{O}$  and  $\delta^2\text{H}$  geochemistry and propose a new conceptual model to explain the global occurrence of  $^{18}\text{O}$  shifts in  $\text{CO}_2$ -rich waters.

In two case studies from Daylesford (Australia) and Pah Tempe (Utah, USA), we investigate the effects of mineral reactions and oxygen isotope exchange with  $\text{CO}_2$  to the observed water oxygen isotope composition. We propose a method to assess the relative contributions of these two mechanisms, which can be applied to waters with elevated  $\text{CO}_2$  concentrations in both natural and engineered settings.

## 2. Oxygen isotope geochemistry in spring waters

### 2.1. Global and local meteoric water lines

The ratios of stable oxygen ( $\delta^{18}\text{O} = ^{18}\text{O}/^{16}\text{O}$ ) and hydrogen ( $\delta^2\text{H} = ^2\text{H}/^1\text{H}$ ) isotopes in water are reported as delta ( $\delta$ ) notation relative to VSMOW (Vienna Standard Mean Ocean Water), following Equation (1), where R represents the  $^{18}\text{O}/^{16}\text{O}$  ratio for the sample and VSMOW, respectively.

$$\delta_{\text{sample}} = \left( \frac{R_{\text{sample}}}{R_{\text{V-SMOW}}} - 1 \right) \times 1000 \quad (1)$$

There is a strong linear relationship between  $\delta^{18}\text{O}$  and  $\delta^2\text{H}$  values in global precipitation reflected by the Global Meteoric Water Line (GMWL), first defined by Craig (1961) and refined by Rozanski et al. (1993):

$$\delta^2\text{H} = 8.2 \times \delta^{18}\text{O} + 11.27 \quad (2)$$

The slope of the line is produced by equilibrium Rayleigh fractionation as precipitation is successively removed from the vapour phase when it condenses, leaving the residual water vapour progressively depleted in  $^{18}\text{O}$  and  $^2\text{H}$ . The intercept of the line is controlled by kinetic fractionation during evaporation of seawater. Variations in humidity and temperature affect the slope and intercept of the line, and produce different Local Meteoric Water Lines (LMWL) for specific locations (Dansgaard, 1964; Clark and Fritz, 1997).

### 2.2. Meteoric water stable isotope change due to natural processes

Various natural processes may deviate the stable isotope ratios in reservoir waters from equilibrium values on the MWLs (Fig. 1). During evaporation, lighter isotopes enter the vapour phase, whereas in condensation heavier isotopes are preferentially incorporated into the condensate. Consequently, water vapour is depleted in  $^{18}\text{O}$  and  $^2\text{H}$  whereas the remaining water is enriched. Similarly, temperature-dependent kinetic fractionation occurs during steam loss above the boiling temperature, which produces  $^{18}\text{O}$  enrichment. (Clark and Fritz, 1997). Fractionation between degassing  $\text{H}_2$ ,  $\text{H}_2\text{S}$ ,  $\text{CH}_4$ , and water in active magmatic systems leads to enriched water  $\delta^2\text{H}$  values without an effect on  $\delta^{18}\text{O}$  (Richet et al., 1977).

$\text{CO}_2$ -rich waters are often characterised by a horizontal deviation from the MWL (e.g. D'Amore and Panichi, 1987; Pauwels et al.,

1997; Cartwright et al., 2000). CO<sub>2</sub> presence in the system can lead to water δ<sup>18</sup>O changes by either:

- i) Promoting low temperature primary mineral dissolution and secondary mineral precipitation reactions, preferentially consuming <sup>18</sup>O.
- ii) Equilibrium oxygen isotope exchange between CO<sub>2</sub> and water.

Both of these processes affect only the water δ<sup>18</sup>O values while δ<sup>2</sup>H values remain unchanged, unless water-rock reactions involve extensive precipitation of H-rich clays (D'Amore and Panichi, 1987). Additionally, diffusive equilibrium oxygen isotope exchange with bedrock minerals at high temperatures produces <sup>18</sup>O-enriched waters. Here, we review and assess the relative contributions of these three processes (Fig. 1) to the observed water δ<sup>18</sup>O values of a global dataset of natural mineral waters.

### 2.2.1. Low temperature dissolution – precipitation reactions

The temperature-dependent oxygen isotope equilibrium fractionation factor between water and a precipitated mineral leads to a preferentially <sup>18</sup>O-enriched mineral phase and lower δ<sup>18</sup>O values of the water. The extent of this enrichment depends on the strength of mineral crystal lattice bonds (Zheng, 2011). Under equilibrium conditions, secondary minerals such as clays and carbonates preferentially incorporate more <sup>18</sup>O during precipitation and hence become enriched relative to the water (Compton et al., 1999; Kloppmann et al., 2002). Clays also incorporate water molecules in the isotopically depleted intra layer, which leads to a positive δ<sup>2</sup>H value shift in the remaining pore water (Sheppard and Gilg, 1996). This process can significantly alter the water δ<sup>18</sup>O if the fraction of oxygen involved in the reactions is sufficiently high (D'Amore and Panichi, 1987). Mineral dissolution and precipitation are particularly important in CO<sub>2</sub>-rich waters, which are often associated with primary silicate hydrolysis and enhanced clay production rates (e.g., Watson et al., 2004; Kampman et al., 2014).

### 2.2.2. Diffusion related equilibrium oxygen isotope exchange with minerals

Meteoric water circulating at depth is depleted in <sup>18</sup>O compared to rock-forming minerals. Oxygen isotope exchange between the fluid and solid phases via diffusion gradually moves the two phases towards equilibrium at a rate controlled by the water temperature. This is important in geothermal systems where the disequilibrium is higher because the fractionation factor between water and minerals is low. In many cases, deep groundwaters are enriched in <sup>18</sup>O relative to the GMWL, with little change in δ<sup>2</sup>H values as a consequence of equilibrium oxygen isotope exchange with bedrock minerals that are commonly low in hydrogen (Clark and Fritz, 1997). However, common rock-forming minerals such as feldspar, mica and quartz require heating to temperatures above 250 °C to achieve this oxygen isotope exchange (D'Amore and Panichi, 1987). Hence the effect is only observed in geothermal conditions (Friedman and O'Neil, 1977).

### 2.2.3. Equilibrium oxygen isotope exchange with CO<sub>2</sub>

Equilibrium oxygen isotope fractionation occurs during redistribution of isotopes between two or more compounds with forward and backward reactions proceeding at equal rates. At isotopic equilibrium heavier isotopes preferentially concentrate in the phase with stronger bond constants (Young et al., 2002). In the case of CO<sub>2</sub> and water, CO<sub>2</sub> has stronger bonds than water and thus equilibrium exchange results in the CO<sub>2</sub> phase being enriched in <sup>18</sup>O. The fractionation factor (α) associated with equilibrium exchange reactions between CO<sub>2</sub> and water is expressed as:

$$\alpha_{\text{CO}_2-\text{H}_2\text{O}} = \frac{\delta^{18}\text{O}_{\text{CO}_2} + 1000}{\delta^{18}\text{O}_{\text{H}_2\text{O}} + 1000} \quad (3)$$

where δ<sup>18</sup>O = <sup>18</sup>O/<sup>16</sup>O at equilibrium relative to VSMOW (Vienna Standard Mean Ocean Water). The fractionation factor α<sub>CO<sub>2</sub>-H<sub>2</sub>O</sub> can be approximated as isotopic enrichment factor ε<sub>CO<sub>2</sub>-H<sub>2</sub>O</sub> expressed as a difference between two reactants (in ‰):

$$10^3 \ln \alpha \approx \epsilon_{\text{CO}_2-\text{H}_2\text{O}} = \delta^{18}\text{O}_{\text{CO}_2} - \delta^{18}\text{O}_{\text{H}_2\text{O}} \quad (4)$$

The fractionation factor is inversely correlated with temperature and is therefore particularly important for low temperature waters (Bottinga, 1968). In most natural systems the oxygen isotope equilibrium between CO<sub>2</sub> and water is predominantly influenced by the initial water δ<sup>18</sup>O value as in the majority of low pressure systems water represents the greater source of oxygen. However, in cases where CO<sub>2</sub> represents a major source of oxygen, the isotopic composition of water may be influenced by CO<sub>2</sub> (e.g., Kharaka et al., 2006; Johnson and Mayer, 2011; Johnson et al., 2011; Serno et al., 2016).

## 2.3. Overview of global CO<sub>2</sub>-rich water isotopic compositions

Observed changes in the oxygen isotope geochemistry of global CO<sub>2</sub>-rich waters have been associated with isotopic equilibrium exchange between natural free phase CO<sub>2</sub> and formation waters (Fig. 2). Examples from the literature include both thermal and cold springs with temperatures similar to those of ambient groundwater. Water <sup>18</sup>O depletion and enrichment without a change in δ<sup>2</sup>H has been observed in cold springs in the Valles Caldera-Southern Jemez Mountains in New Mexico, USA (Vuataz and Goff, 1986), along the Bongwana gas fault in South Africa (Harris et al., 1997) and in shallow boreholes in the Mont-Dore and Montmiral regions of the Massif Central, France (Casanova et al., 1999; Humez et al., 2014; Pauwels et al., 1997, 2007). The Alto Guadalentín groundwater aquifer in southeast Spain showed a similar shift in δ<sup>18</sup>O which has been associated with the manifestation of CO<sub>2</sub> from greater depth due to overexploitation of the aquifer, and oxygen isotope equilibrium exchange between the CO<sub>2</sub> gas and reservoir water (Cerón et al., 1998; Cerón and Pulido-Bosch, 1999). Geochemical differences in various northern Portuguese CO<sub>2</sub>-rich mineral waters are reportedly caused by water-CO<sub>2</sub> isotopic equilibrium exchange (Marques et al., 2000). A majority of the bubbling pools in the central Italian volcanic region, and some hydrothermal waters from Sicily, exhibit a δ<sup>18</sup>O value deviation from the Local Meteoric Water Line (LMWL), which is likely the result of oxygen isotope exchange between the meteoric water and CO<sub>2</sub> (Cinti et al., 2011).

A comparative study of thermal and cold spring waters in the Poroto-Rungwe region in Tanzania revealed that springs with observed sustained CO<sub>2</sub> flux show water <sup>18</sup>O depletion of up to -8‰ relative to the LMWL, while springs with relatively lower and episodic bubbling gas emanations are isotopically similar to surface meteoric water. Water <sup>18</sup>O depletion was negatively correlated with temperature (Delalande et al., 2011), consistent with experimental observations indicating fractionation increase at low temperatures (Bottinga, 1968). Water <sup>18</sup>O depletion caused by mantle-derived CO<sub>2</sub> interaction with cold springs is also observed at the Snæfellsnes Peninsula in Iceland. A number of hot springs from the same region are <sup>18</sup>O enriched, although this is interpreted as a result of isotopic exchange with bedrock minerals at geothermal temperatures (Thomas et al., 2016). Finally, evidence from Hofsstadir (Iceland) shows that the effect of oxygen isotope exchange can be preserved in water after the gas has leaked out of

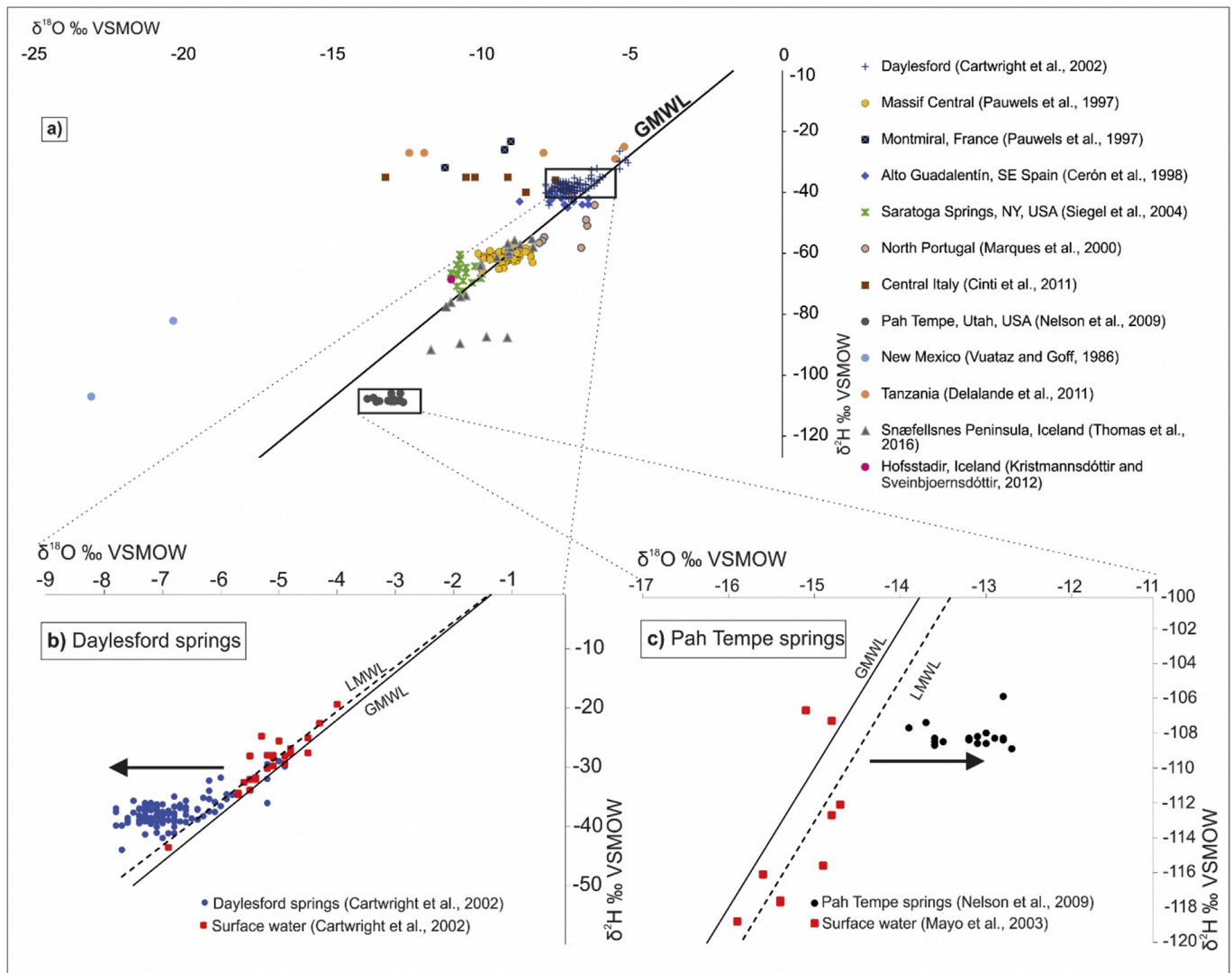


**Fig. 2.** a) Global compilation of  $\text{CO}_2$ -rich waters showing  $^{18}\text{O}$  depletion or enrichment without a change in  $\delta^2\text{H}$  values relative to the GMWL. b) Daylesford: compilation of water isotopic composition in mineral spring waters, previously published by Cartwright et al. (2002).  $\delta^{18}\text{O}$  values of spring waters are lower by as much as 1.43‰ relative to the LMWL. c) Pah Tempe:  $\delta^{18}\text{O}$  values of spring waters are higher than respective values on the LMWL (Kendall and Coplen, 2001) by up to 1.68‰ (data from Nelson et al., 2009). Full dataset is available as [supplementary Table A](#).

the system. Stagnant geothermal water pools with low  $\text{CO}_2$  contents are reportedly depleted in  $^{18}\text{O}$  due to an episode of  $\text{CO}_2$  flux in the past (Kristmannsdóttir and Sveinbjörnsdóttir, 2012). Hence, this global compilation of observed  $\text{CO}_2$ -rich water oxygen isotope composition clearly shows that  $^{18}\text{O}$  depletion or enrichment without a change in  $\delta^2\text{H}$  is a common feature of low temperature  $\text{CO}_2$ -rich springs and groundwaters and can be associated with both actively degassing and previously degassed systems. Strong horizontal trend in deviations from  $\delta^{18}\text{O}$  values suggest this process is separate to the change in  $\delta^2\text{H}$  values relative to current surface waters, which is attributed to recharge at different temperatures.

In our study, we focus on two natural examples of  $\text{CO}_2$ -rich springs showing opposing linear  $\delta^{18}\text{O}$  deviations from the MWL.  $\text{CO}_2$ -rich mineral springs in Daylesford, south east Australia, show water stable isotope values ranging from  $-7.8$  to  $-5.8$ ‰ for  $\delta^{18}\text{O}$  and  $-44$  to  $-31.8$ ‰ for  $\delta^2\text{H}$ , and are depleted in  $^{18}\text{O}$  relative to the LMWL by up to 1.43‰ (Fig. 2b). Cartwright et al. (2002) attributed this to interaction with  $\text{CO}_2$  and degassing at the surface. In contrast, Pah Tempe mineral waters in Utah, USA, range between 25 and 27.1‰ for  $\delta^{18}\text{O}$  and  $-108.9$  to  $-105.9$ ‰ for  $\delta^2\text{H}$ , and are

enriched in  $^{18}\text{O}$  compared to the LMWL by up to 1.68‰ (Fig. 2c).

The mechanism of water  $^{18}\text{O}$  enrichment at Pah Tempe is currently uncertain. Nelson et al. (2009) suggested equilibrium isotope exchange with bedrock minerals at temperatures above  $150$  °C on the basis of the lack of other plausible mechanism for water  $^{18}\text{O}$  enrichment. However, evidence for  $>3$ – $5$  km deep faults providing circulation pathways is limited (Nelson et al., 2009) and the temperature of the water discharging at the surface ranges from  $39$  to  $41$  °C (Dutson, 2005). Further, circulation temperatures calculated from other conventional geothermometry techniques indicate lower temperatures:  $70$ – $75$  °C using conductive and adiabatic silica and  $37$ – $39$  °C using chalcedony silica geothermometers (Dutson, 2005) and up to  $80$  °C using quartz and Na-K-Ca-Mg geothermometer (Budding and Sommer, 1986).

### 3. Geological background of case studies

#### 3.1. Daylesford springs, Australia

Daylesford mineral springs are located in the Central Highlands

of Victoria, south east Australia (Fig. 3a). There are more than 100 low temperature CO<sub>2</sub>-rich springs in the area, which have been exploited historically for drinking and recreational purposes. Springs flow in a fracture-dominated aquifer through an Ordovician

turbidite sequence altered to greenschist facies and discharge into topographic lows such as streambeds. The depth of circulation is unknown but historical records report spring water in mines at a maximum depth of 1.6 km (Shugg, 2009). The aquifer is overlain by

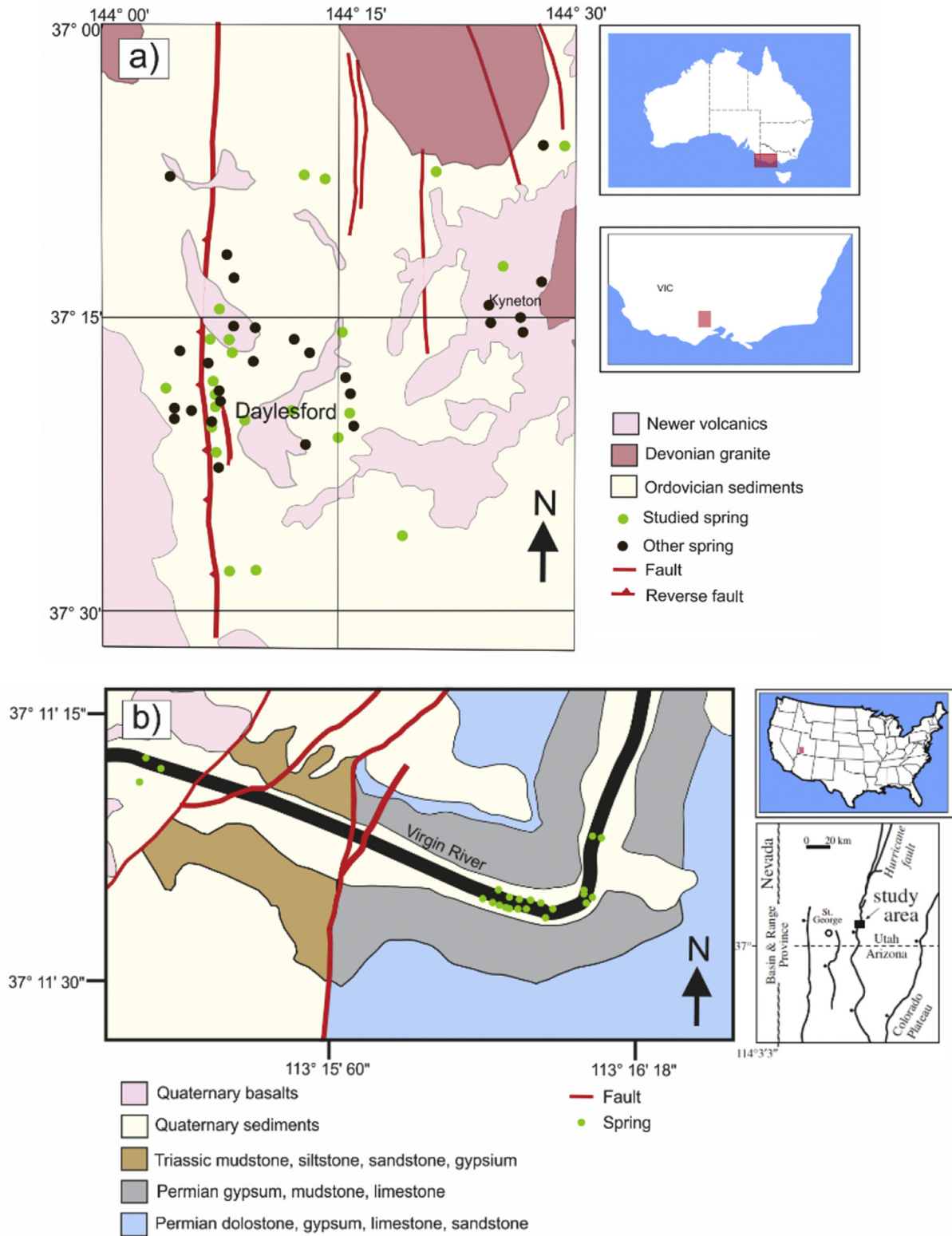


**Fig. 3.** a) Location map of Daylesford springs in Victoria, SE Australia. Springs emanate near major fault lines and Newer Volcanic eruption centres (adapted from Cartwright et al., 2002). b) Pah Tempe springs in Utah, USA. Springs discharge into the stream bed of Virgin River in a close proximity to the Hurricane fault (adapted from Nelson et al., 2009).

Newer Volcanic basalts, active from 4.5 Ma to 5000 a (Boyce, 2013). The spring waters contain excess dissolved carbon (Weaver et al., 2006) and actively degasses at surface discharge points. CO<sub>2</sub> is reportedly mantle-sourced, based on their close proximity to the eruptive centres (Lawrence, 1969), <sup>3</sup>He/<sup>4</sup>He gas data (Chivas et al., 1983), and gas carbon isotope values (δ<sup>13</sup>C; Cartwright et al., 2002). Spring waters are Na-HCO<sub>3</sub> type with a significant solute composition variation between individual springs (Weaver et al., 2006).

### 3.2. Pah Tempe springs, Utah, USA

The Pah Tempe springs discharge in the damage zone of the currently active Hurricane fault at Timpoweap Canyon, Utah, USA (Fig. 3b). The Hurricane fault has a total displacement of up to 3000 m and a 200 m wide core (Biek, 2003). All springs discharge at the eastern damage zone into the Virgin River Canyon. The stratigraphic sequence includes Cretaceous sandstones, siltstones and shales, and carbonaceous Jurassic – Triassic sediments and evaporites (Biek, 2003; Nelson et al., 2009). Free-phase CO<sub>2</sub> is actively degassing at the surface, forming prominent bubble trains, along with mineralised water at an elevated temperature of 40 °C. The spring waters are high in Na<sup>+</sup>, Cl<sup>-</sup>, Ca<sup>2+</sup> and SO<sub>4</sub><sup>2-</sup> as well as dissolved CO<sub>2</sub> (Dutson, 2005). Helium isotope and δ<sup>13</sup>C analysis indicate carbonate thermal alteration as a primary CO<sub>2</sub> source (Nelson et al., 2009).

## 4. Methods

### 4.1. CO<sub>2</sub> sampling

CO<sub>2</sub> samples from Daylesford and Pah Tempe springs were collected using a funnel placed over a bubbling vent and connected by plastic hosing to a copper tube. After purging air from the sampling line by allowing gas to flow for 5–10 min, the copper tubes were sealed by two metal clamps at either side creating a helium leak tight cold weld. At Daylesford water samples were collected via hand pumping the mineral water wells and from stream waters at gas discharge locations where CO<sub>2</sub> samples were collected. Waters were filtered through 0.45 μm pore-size filters and filled into Nalgene bottles (with no headspace) or vacutainers. Samples were stored in a cooler until analysis to avoid evaporation. The temperature of the water which the CO<sub>2</sub> was bubbling through was measured in the field using a Hannah Instruments HI991300 Portable Waterproof pH/EC/TDS Meter. Temperature accuracy is ±0.5 °C.

### 4.2. Stable isotope analysis

The δ<sup>18</sup>O values of exsolved CO<sub>2</sub> gas samples from Pah Tempe and Daylesford were measured at the Scottish Universities Environmental Research Centre (SUERC). Gas samples were released into an ultra-high vacuum extraction line. Two aliquots of the gas were trapped into glass ampules for stable isotope analysis, using liquid nitrogen and sealing the ampule with a blowtorch after pumping away the other volatile gases. Samples were analysed using a VG Isotech Sira 2b mass spectrometer with typical uncertainties of ±0.3‰. δ<sup>18</sup>O and δ<sup>2</sup>H measurements of two Daylesford water samples were obtained at the University of Wollongong, School of Earth and Environmental Sciences Stable Isotope laboratory using a Micromass PRISM III mass spectrometer. Uncertainties for δ<sup>18</sup>O and δ<sup>2</sup>H measurements are ±0.1‰ and ±1‰ respectively.

### 4.3. Numerical simulation of water-rock reactions

Numerical simulations allow the quantification of the mass transfer between the solid and fluid phases during dissolution and precipitation reactions at elevated CO<sub>2</sub> pressures. The amount of oxygen liberated from dissolving minerals and precipitated in secondary minerals can be compared to the total oxygen in the solution to assess the contribution of water-rock reactions to the overall water oxygen isotope signature.

Mineral dissolution and precipitation reactions are simulated using the geochemical modelling software PHREEQC (Parkhurst and Appelo, 1999) with the WATEQ4F database (Ball and Nordstrom, 1991). The numerical simulations solve a set of nonlinear mass balance equations using thermodynamic constants defined in the database.

Simulations require a set of reactive primary and precipitating secondary minerals, which are chosen according to the saturation indices of the dissolved species in groundwater calculated in PHREEQC and the geology of the local areas. The main goal of the simulations was to reproduce the observed geochemistry of the spring waters, published in Weaver et al. (2006) for Daylesford springs and Dutson (2005) for Pah Tempe springs, and to quantify the oxygen isotope transfer between the solid and fluid phases. There are multiple reaction pathways to achieve the observed water chemistry but the model seeks to represent the simplest solution using the most likely reactive phases based on the geological setting.

#### 4.3.1. Model assumptions

**4.3.1.1. Initial groundwater and CO<sub>2</sub> dissolution.** Equilibrium dissolution and precipitation reactions are modelled in a closed system considering reactive species in 1 L of water. Average modern local groundwater is used as a starting solution (Table 1). CO<sub>2</sub> partial pressure (pCO<sub>2</sub>) is calculated from measured pH and alkalinity (as HCO<sub>3</sub><sup>-</sup>) values, so mineral reactions are modelled at ambient pressures and average recorded spring discharge temperatures (25 and 40 °C for Daylesford and Pah Tempe, respectively). This method provides the best fit to the measured DIC contents. Alternatively, reactions could be modelled at depth with higher pCO<sub>2</sub> and subsequent dilution at the surface. This would allow dissolution of more stable minerals in the beginning (May 2005) but was found not to have a significant effect on the overall mass balance.

**4.3.1.2. Mineral reactions in Daylesford, Australia.** Major cation concentrations and bicarbonate contents display a positive correlation, indicating that mineral dissolution is proportional to acid neutralisation. This is a common feature in Na-Ca-HCO<sub>3</sub> type waters produced by acid groundwater dissolution of silicates (May 2005). These trends infer that the bulk reaction is limited by the kinetics of primary mineral dissolution and that the system is not in equilibrium. SiO<sub>2</sub> does not show correlation with HCO<sub>3</sub><sup>-</sup>, suggesting secondary silica precipitation.

The model assumes reactions with common minerals in the Ordovician Castlemaine turbidite sequence and Newer Volcanics intrusions. Albite and chlorite were chosen as source rocks for Na, Mg and Fe in the water based on XRD analysis of average Ordovician Castlemaine turbidites collected in the Ballarat area (Bierlein et al., 1999). The study compares unaltered Ordovician rock with that altered by hydrothermal fluids. Two other major phases, muscovite and quartz, are stable at hydrothermal conditions, and therefore are assumed to be unreactive in CO<sub>2</sub>-water system in the model. Ca and small amounts of K are sourced from feldspars in mafic Ca-rich and trachytic lavas from the Newer Volcanic sequence (Price et al., 2003), and are modelled as anorthite and adularia. Dissolution of minor amounts of sulfates (melanterite, barite) contributes SO<sub>4</sub>, Fe

**Table 1**

Baseline water compositions. Daylesford: weighted average Melbourne precipitation water between 2007 and 2011 (Crosbie et al., 2012). Pah Tempe: average Virgin River valley groundwater 2015 (Burden, 2015).

	pH	Total Alk. meq/L	Cl <sup>-</sup> mg/L	SO <sub>4</sub> <sup>2-</sup> mg/L	Ca <sup>2+</sup> mg/L	K <sup>+</sup> mg/L	Mg <sup>2+</sup> mg/L	Na <sup>+</sup> mg/L
Daylesford	5.85	0.12	5.36	1.76	1.14	0.48	0.42	3.11
Pah Tempe	7.01	0.88	23.3	2.3	81.7	3	20	25.6

and Ba to the system, consistent with redox values measured by Weaver et al. (2006). Other trace elements (Sr, Mn) are sourced from carbonate dissolution (rhodochrosite, siderite). Secondary minerals are allowed to precipitate to equilibrium were kaolinite, amorphous silica and Mg-carbonates.

**4.3.1.3. Mineral reactions in Pah Tempe, Utah, USA.** The main model assumptions are based on spring water geochemistry interpretation by Dutson (2005). There is little variation in solute contents between samples collected at different discharge sites (Dutson, 2005), suggesting springs emerge from a single aquifer. The average molar ratios for Na/Cl and Ca/SO<sub>4</sub> are 1.08 and 0.98, indicating halite and gypsum dissolution, which could be sourced from the Triassic sequence (Biek, 2003; Dutson, 2005). As gypsum accounts for most of the Ca contents, carbonate dissolution is unlikely. Minor amounts of Mg and K are introduced by silicate dissolution, modelled as phlogopite. Precipitation of amorphous silica provides a sink for Si.

## 5. Results

### 5.1. Stable isotope composition

Oxygen isotope ratios of CO<sub>2</sub> ( $\delta^{18}O_{CO_2}$ ) degassing at the surface of spring discharge points in Daylesford are 36.3‰ and 34.1‰. The water sampled near gas flux points has  $\delta^{18}O$  values of -6.3‰ and -5.55‰ and  $\delta^2H$  values of -34.6‰ and -33.1‰.  $\delta^{18}O_{CO_2}$  values of two Pah Tempe springs are 25‰ and 26.8‰ (Table 2).

### 5.2. Low temperature mineral precipitation – dissolution reactions

Numerical simulations of equilibrium dissolution and precipitation of primary and secondary phases at fixed CO<sub>2</sub> partial pressures (0.8 atm in Daylesford and 0.79 atm in Pah Tempe) produce geochemical compositions that closely match the reported measurements of Na-HCO<sub>3</sub> and Na-Cl-HCO<sub>3</sub> waters from Daylesford and Pah Tempe (Fig. 4). In Daylesford, the modelled Na, Ca, K, SO<sub>4</sub> and trace element (Fe, Sr, Mn and Ba) contents are fixed by the defined amount of primary dissolving minerals, while Mg and Si concentrations are controlled by equilibrium secondary mineral precipitation. For Pah Tempe springs, Na, Cl, Mg and K contents are controlled by fixed amounts of mineral dissolution, Ca and SO<sub>4</sub> are limited by the gypsum solubility, and Si is controlled by the kaolinite and secondary silica precipitation. Both models overestimate Si contents. The exact precipitating silica polymorphs are unknown and the thermodynamic constant for amorphous silica used in the simulation may not be precise. The relative amounts of dissolving minerals are not proportional to the bulk rock

composition (as reported by Bierlein et al., 1999) suggesting that carbonic acid alteration is limited by mineral dissolution kinetics. The modelling approach for which fixed amounts of minerals are dissolved to match the observed element concentrations effectively eliminates the uncertainties associated with predicting individual mineral dissolution rates.

The total amount of phases that react are summarised in Table 3. In both cases, mineral reactions liberate more oxygen to the system than remove via precipitation. However, the total amount of oxygen involved in both types of reactions represents only 0.11% and 0.087% of total oxygen atoms in the water in Daylesford and Pah Tempe, respectively.

## 6. Discussion

### 6.1. Water – rock reaction influence to water oxygen isotope composition

The effect of mineral dissolution and precipitation on the water oxygen isotope composition depends on the  $\delta^{18}O$  values of the water, dissolving and precipitating phases, and the relative ratios between the solid and fluid phases. This relationship can be expressed by a simple mass balance model:

$$X_m^o \times \delta^{18}O_m^i + X_w^o \times \delta^{18}O_w^i = X_m^o \times \delta^{18}O_m^f + X_w^o \times \delta^{18}O_w^f \quad (5)$$

Where  $X^o$  is the relative fraction of oxygen in the phase, and  $\delta^{18}O^i$  and  $\delta^{18}O^f$  are the initial and final oxygen isotope ratios in mineral ( $m$ ) and water ( $w$ ). The mass balances obtained from numerical simulations (Table 3) indicate that mineral reactions account for dissolution of 0.7 g and 0.8 g, and precipitation of 0.4 g and 0.04 g of oxygen per 1 L of water in Daylesford and Pah Tempe, respectively. This represents ~0.1% of the total oxygen in the water. The theoretical water  $\delta^{18}O$  change in Daylesford and Pah Tempe given a  $\delta^{18}O$  range of viable rock forming mineral values (5–40‰) does not exceed 0.01‰, which is below the analytical sensitivity and therefore has a negligible influence on the  $\delta^{18}O$ .

It is also important to consider mineral reactions that achieve equilibrium quickly and may not be evident in the water geochemistry, such as primary carbonate dissolution and secondary carbonate precipitation. A theoretical scenario of carbonate dissolution with low  $\delta^{18}O$  values formed at high temperatures and re-precipitation at low temperatures would result in a water  $^{18}O$  depletion of 0.5‰, requiring progressive reworking of 200 g of carbonates per 1 L of water. A recent study by Sterpenich et al. (2009) demonstrated that less than 1% by mass of an oolitic limestone dissolved due to interaction with CO<sub>2</sub>-saturated water under extreme experimental conditions (150 bar, 80 °C). These results

**Table 2**

$\delta^{18}O_{CO_2}$ ,  $\delta^{18}O_{H_2O}$ ,  $\delta^2H$  and temperature values for mineral water gas discharges collected in Daylesford and Pah Tempe.

Location	Spring ID	$\delta^{18}O_{H_2O}$ ‰ VSMOW	$\delta^2H$ VSMOW	$\delta^{18}O_{CO_2}$ ‰ VSMOW	T °C
Daylesford	Locarno	-6.30	-34.6	36.3	16.7
Daylesford	Taradale	-5.55	-33.1	34.1	20.9
Pah Tempe	Virgin No4.7110106			25	
Pah Tempe	PAH TEMPE 1.B			26.8	

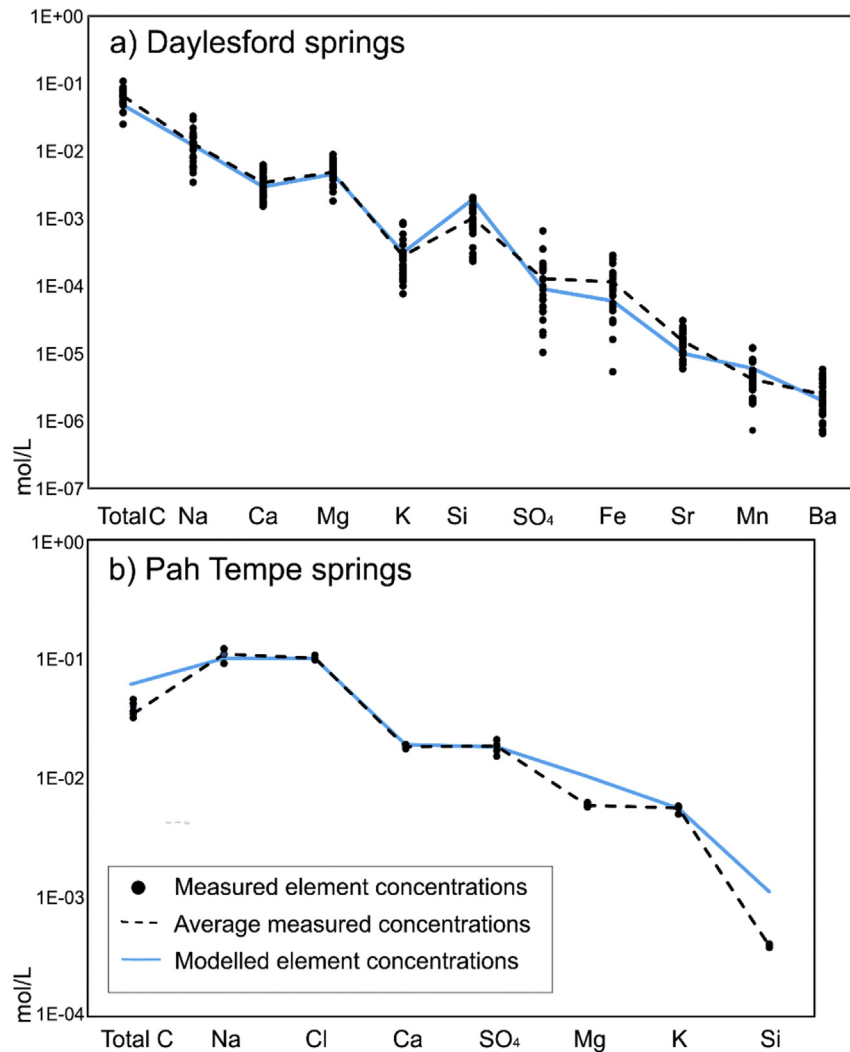


**Fig. 4.** Geochemical modelling results compared to average concentrations from the literature. a) Molality in solution at 25 °C in Daylesford b) Pah Tempe springs (40 °C). Black dots represent measured values reported by [Weaver et al. \(2006\)](#) for Daylesford and [Dutson \(2005\)](#) for Pah Tempe springs. The dashed black line is an average of the measured values. The blue solid line shows modelled element concentrations. (For interpretation of the references to colour in this figure legend, the reader is referred to the web version of this article.)

clearly show that carbonate dissolution and re-precipitation at the amounts required to significantly alter  $\delta^{18}\text{O}$  values is unlikely.

The mineral water geochemistry in Daylesford and Pah Tempe is controlled by the primary mineral dissolution and secondary mineral precipitation accelerated by elevated  $\text{CO}_2$  partial pressures. However, the fraction of oxygen in these reactions is too small to influence the oxygen isotope ratio of the water body. Consequently, water-rock reactions cannot account for water  $\delta^{18}\text{O}$  deviations from the LMWL in both case studies due to their low salinity. However, the method could be applicable to more saline formations where mineral reaction may liberate enough oxygen to alter water  $\delta^{18}\text{O}$  values, such as deep basement fluids and hypersaline brines. Depletion of  $^{18}\text{O}$  in saline brines (up to 250 g/L) in Fennoscandian and Canadian Shields have been previously interpreted as a result of low temperature water-rock reactions ([Blomqvist, 1990](#); [Frape and Fritz, 1982](#)).

## 6.2. $\text{CO}_2$ -water oxygen isotope exchange influence on water isotopic composition

Our geochemical modelling results clearly show that low

temperature mineral reactions can be excluded as a significant source of oxygen to the waters at Daylesford and Pah Tempe. Hence these two case studies, along with the global compilation of stable isotope values from  $\text{CO}_2$ -rich springs, provide robust evidence that  $\text{CO}_2$ -water oxygen isotope equilibrium exchange in the subsurface can result in  $^{18}\text{O}$  depletion and enrichment in  $\text{CO}_2$ -rich spring waters compared to the MWL.

The amount of  $\text{CO}_2$  required to achieve the  $\delta^{18}\text{O}_{\text{H}_2\text{O}}$  change observed in Daylesford ( $-1.43\text{‰}$ ) and Pah Tempe ( $1.68\text{‰}$ ) can be estimated using the conceptual model developed by [Johnson et al. \(2011\)](#). The magnitude of the shift in  $\delta^{18}\text{O}_{\text{H}_2\text{O}}$  relates to the fraction of  $\text{CO}_2$  in the system. The extent to which  $\text{CO}_2$  can change the oxygen isotope composition of reservoir water depends on the:

- Initial  $\delta^{18}\text{O}_{\text{CO}_2}$
- Initial water  $\delta^{18}\text{O}$  value ( $\delta^{18}\text{O}_{\text{H}_2\text{O}}$ ) calculated from the LMWL
- Relative proportions of  $\text{CO}_2$  and water that equilibrate ( $X_{\text{CO}_2}^0$  as the fraction of oxygen sourced from  $\text{CO}_2$  in the system)
- Temperature-dependent oxygen isotope enrichment factor ( $\epsilon_{\text{CO}_2-\text{H}_2\text{O}}$ )

**Table 3**

Summary of dissolving and precipitating minerals in Daylesford and Pah Tempe springs, and associated oxygen concentrations contributing to the water. Oxygen sourced from mineral reactions is compared to the total oxygen atoms in 1 L of water (55.6 mol/L).

Phase		Dissolved mol/L	Precipitated mol/L	O dissolved mol/L	O precipitated mol/L
<b>Daylesford springs</b>					
Adularia	KAlSi <sub>3</sub> O <sub>8</sub>	3.00E-04		1.85E-04	
Albite	NaAlSi <sub>3</sub> O <sub>8</sub>	1.20E-02		7.38E-03	
Anorthite	CaAl <sub>2</sub> Si <sub>2</sub> O <sub>8</sub>	4.00E-03		2.46E-03	
Barite	BaSO <sub>4</sub>	2.00E-06		1.33E-06	
Celestite	SrSO <sub>4</sub>	1.00E-05		6.67E-06	
Chlorite	(Mg,Fe) <sub>3</sub> (Si,Al) <sub>4</sub> O <sub>10</sub>	9.00E-04		3.75E-04	
CO <sub>2(g)</sub>	CO <sub>2</sub>	4.67E-02		3.11E-02	
Melanterite	FeSO <sub>4</sub> ·7H <sub>2</sub> O	6.00E-05		2.44E-05	
Rhodochrosite	MnCO <sub>3</sub>	6.00E-06		3.60E-06	
Dolomite	CaMg(CO <sub>3</sub> ) <sub>2</sub>		1.31E-03		7.85E-04
Kaolinite	Al <sub>2</sub> Si <sub>2</sub> O <sub>5</sub> (OH) <sub>4</sub>		1.11E-02		5.85E-03
Amorphous silica	SiO <sub>2</sub>		2.36E-02		1.57E-02
<b>Total</b>		<b>0.06</b>	<b>0.04</b>	<b>0.04</b>	<b>0.02</b>
<b>% of total O in 1 L of water</b>					
<b>Pah Tempe springs</b>					
CO <sub>2(g)</sub>	CO <sub>2</sub>	5.54E-02		3.69E-02	
Gypsum	CaSO <sub>4</sub> ·2H <sub>2</sub> O	1.91E-02		9.53E-03	
Halite	NaCl	1.00E-01		0	
Phlogopite	KMg <sub>3</sub> (AlSi <sub>3</sub> O <sub>10</sub> )(F,OH) <sub>2</sub>	2.00E-03		1.00E-03	
Amorphous silica	SiO <sub>2</sub>		2.39E-03		1.59E-03
<b>Total</b>		<b>0.18</b>	<b>0.002</b>	<b>0.047</b>	<b>0.002</b>
<b>% of total O in 1 L of water</b>					
				<b>0.085</b>	<b>0.003</b>

This relationship is expressed in equation (6) where  $\delta^{18}O_{H_2O}^f$  is the final oxygen isotope composition of water (Johnson et al., 2011):

$$\delta^{18}O_{H_2O}^f = (\delta^{18}O_{CO_2}^i - \epsilon_{CO_2-H_2O}) \times X_{CO_2}^O + \delta^{18}O_{H_2O}^i \times (1 - X_{CO_2}^O) \quad (6)$$

The CO<sub>2</sub> source determines the initial  $\delta^{18}O_{CO_2}^i$ , which is an important control on the ultimate water  $\delta^{18}O$  shift achieved at equilibration. Generally,  $\delta^{18}O$  values in rocks decrease with increasing formation temperature (Fig. 5). Due to this difference of initial values, mantle CO<sub>2</sub> has the potential to produce the most <sup>18</sup>O-depleted fluids after equilibration, while CO<sub>2</sub> generated through thermal carbonate alteration may enrich water in <sup>18</sup>O.

In Daylesford we consider two examples of  $\delta^{18}O_{CO_2}^i$  values associated with mantle degassing. The first one (8‰) represents a 'minimum value' scenario of CO<sub>2</sub> degassed from a volcanic source whereby large amounts of mantle-sourced gas ascends through the crust without significant interaction with fluids other than the mineral springs. However,  $\delta^{18}O$  is likely to change due to the interaction with subsurface fluids with increasing migration or residence time in a natural trap. The second scenario represents mantle CO<sub>2</sub> after interaction with subsurface fluids and uses  $\delta^{18}O$  value of 19.1‰ measured in Caroline CO<sub>2</sub> field in Mt. Gambier, South Australia (Chivas et al., 1987), which is associated with the same period of volcanic activity as the eruptive centres in Daylesford. A  $\delta^{18}O_{CO_2}^i$  value of 30‰ represents an average value for thermogenic CO<sub>2</sub> from a global range (Bindeman, 2008). Equilibration with these potential values for mantle-derived CO<sub>2</sub> at Daylesford would require the fraction of oxygen sourced from CO<sub>2</sub> in the system ( $X_{CO_2}^O$ ) to be 5% and 10% for average mantle and Caroline field CO<sub>2</sub>, respectively, to explain the maximum observed  $\delta^{18}O$  deviations. The maximum  $\delta^{18}O$  shift observed in Pah Tempe can be explained by equilibration with the average thermogenic CO<sub>2</sub> when  $X_{CO_2}^O$  is 30%. This amounts to 60–120 g and 366 g of CO<sub>2</sub> per every litre of water in Daylesford and Pah Tempe, respectively.

This simple model uses a closed system two-component mixing approach. In reality, both CO<sub>2</sub> and water move through the system at different rates. If CO<sub>2</sub> moves through a relatively stagnant water

body at a continuous rate and degasses at the surface, the calculated  $X_{CO_2}^O$  ranges represent the amount of CO<sub>2</sub> that the water has interacted with, rather than the amount of CO<sub>2</sub> currently present in the system. Therefore, these values can be taken as a maximum estimate.

The variation of oxygen isotope ratios in MORB-type igneous rocks are between 5.5 and 5.9‰, rhyolitic magmas have values between 5.8 and 6.5‰ and the overall range of various measured igneous lithologies is 4–12‰ (Fig. 5 inset) (Bindeman, 2008). CO<sub>2</sub>-mineral isotopic enrichment factors measured at melting temperatures range between 2 and 6‰ (Matthews et al., 1994), giving the overall range of volcanic degassing related  $\delta^{18}O_{CO_2}^i$  values of 6–18‰ with MORB-like signatures at the lower end of the spectrum. In contrast,  $\delta^{18}O$  values of sedimentary and carbonate rocks range between 8 and 32‰. CO<sub>2</sub>-mineral isotopic enrichment factors span from 2 to 11‰ depending on temperature and are at the higher end of this spectrum in temperatures relevant to thermogenic gas generation (Zheng, 1999; Zhao and Zheng, 2003). Considering the fact that meteoric water  $\delta^{18}O$  values span from –65 to 0‰ and the wide range of natural  $\delta^{18}O_{CO_2}^i$  values, it is clear that oxygen isotope exchange with CO<sub>2</sub> can both deplete or enrich water in <sup>18</sup>O within the range of naturally occurring  $\delta^{18}O_{CO_2}^i$  and  $\delta^{18}O_{H_2O}$  values, as demonstrated using the case studies from Daylesford and Pah Tempe.

### 6.3. Differences between observed and theoretical enrichment factors

We combine newly obtained gas  $\delta^{18}O_{CO_2}$  and water  $\delta^{18}O_{H_2O}$  measurements with those previously published in Dutson (2005) to calculate the expected oxygen isotope enrichment factor ( $\epsilon_{CO_2-H_2O}$ ) (Bottinga, 1968) for individual springs (Table 4). For Pah Tempe springs calculations, we use an average temperature for springs where data is not available and  $\delta^{18}O_{CO_2}$  value of  $26.3 \pm 0.9$ ‰, which is an average of two measurements reported in this paper and one measurement of 27.1‰ reported in Dutson (2005). Temperature-dependent oxygen isotope enrichment factors  $\epsilon_{CO_2-H_2O}$  calculated for the individual springs are larger than

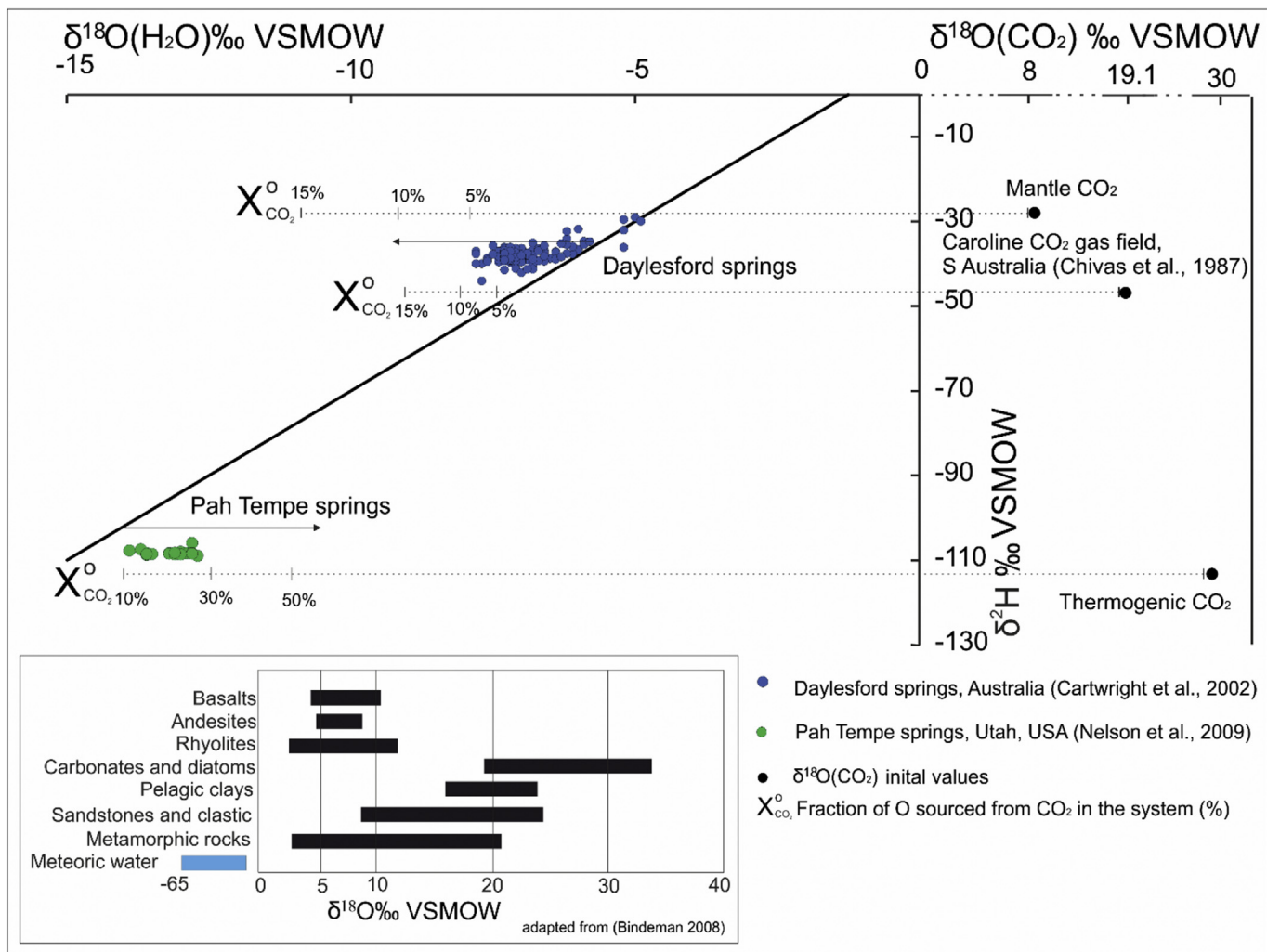


**Fig. 5.** Water samples from Daylesford (blue) and Pah Tempe (green) showing  $\delta^{18}\text{O}$  deviations from the GMWL. The additional graph on the right shows potential initial  $\delta^{18}\text{O}_{\text{CO}_2}$  values the water could have equilibrated with. The dashed lines with percentages show the  $X_{\text{CO}_2}^0$  required to produce the observed shift for the chosen examples. Average mineral  $\delta^{18}\text{O}$  values provided in the inset at the bottom left (adapted from Bindeman, 2008). (For interpretation of the references to colour in this figure legend, the reader is referred to the web version of this article.)

the observed difference between  $\delta^{18}\text{O}$  of water and  $\text{CO}_2$  ( $\Delta$ ) in all cases except for Taradale spring in Daylesford. The difference between the observed and theoretical enrichment factor ( $\Delta - \epsilon$ ) is 0.2‰ and  $-1.9\text{‰}$  for two Daylesford springs and  $2 \pm 0.4\text{‰}$  for Pah Tempe. Potential reasons for this apparent dis-equilibrium include the effects of salinity, partial equilibrium during  $\text{CO}_2$  ascent and kinetic fractionation on bubble surfaces. These mechanisms have opposing isotopic effects: bubble formation on the surface leads to lower apparent  $\text{CO}_2$ -water fractionation factor, while salinity and partial equilibration can either decrease or increase it.

### 6.3.1. Water salinity

High salinity waters display slightly altered  $\epsilon_{\text{CO}_2-\text{H}_2\text{O}}$  depending on temperature and total dissolved solids (TDS). Truesdell (1974) and Becker et al. (2015) reported  $\epsilon_{\text{CO}_2-\text{H}_2\text{O}}$  decreasing by 1‰ in laboratory experiments using NaCl solutions of up to 250 g/L. Lécuyer et al. (2009) reported an increase in fractionation factor by up to 0.5‰ for 250 g/L KCl and sea salt solutions, which highlights the fact that different types of ions may have opposing effects. Given the relatively low salinities at Pah Tempe (8 g/L) (Dutson, 2005) and Daylesford (5 g/L) (Cartwright et al., 2002), this effect should be negligible.

### 6.3.2. Partial equilibration during $\text{CO}_2$ ascent to the surface

$\text{CO}_2$ -water isotopic equilibrium established locally or at a certain depth may be affected by the kinetics of two-phase fluid flow as  $\text{CO}_2$  ascends to the surface. The extent of mixing achieved by  $\text{CO}_2$  and water depends on the nature of interaction at depth. The observed water  $\delta^{18}\text{O}$  shift requires large quantities of free phase  $\text{CO}_2$  interacting with the water. There is significant heterogeneity associated with the two-phase  $\text{CO}_2$  and water flow through the subsurface due to pressure and temperature effects on  $\text{CO}_2$  physical properties.  $\text{CO}_2$  and water may interact as transient, dispersed or separated two-phase flows at varying rates, depending on bedrock properties and interfacial tensions between the two phases (Plampin et al., 2014; Roberts et al., 2015). As pressure and temperature decrease at shallow levels of the subsurface, increased  $\text{CO}_2$  buoyancy provides a driving force to migrate at a faster rate.  $\text{CO}_2$  may achieve local equilibrium with surrounding water at depth where the flow rate is relatively low and where the isotopic signature is preserved after rapid ascent to the surface. Consequently, the remaining water will re-equilibrate and display a smaller  $\delta^{18}\text{O}$  shift than expected if in equilibrium with the sampled  $\text{CO}_2$ . This may be the case in Pah Tempe springs where the  $\text{CO}_2$  flux is strong and sustained - measured  $\delta^{18}\text{O}_{\text{CO}_2}$  may represent

**Table 4**

Summary of temperature and isotope measurement data in Pah Tempe and Daylesford springs used to calculate theoretical ( $\epsilon_{\text{CO}_2-\text{H}_2\text{O}}$ ) and observed enrichment factors ( $\Delta \approx \delta^{18}\text{O}_{\text{CO}_2} - \delta^{18}\text{O}_{\text{H}_2\text{O}}$ ). The observed enrichment factor  $\Delta \approx \delta^{18}\text{O}_{\text{CO}_2} - \delta^{18}\text{O}_{\text{H}_2\text{O}}$  is calculated as  $\Delta = 1000 \ln \alpha$ ;  $\alpha = (\delta^{18}\text{O}_{\text{CO}_2} + 1000) / (\delta^{18}\text{O}_{\text{H}_2\text{O}} + 1000)$ . All temperature and water isotope data from Pah Tempe springs from Dutson (2005).  $\delta^{18}\text{O}_{\text{CO}_2}$  value for Pah Tempe springs an average from 2 measurements reported in this paper (Table 2) and one measurement (27.1‰) from Dutson (2005). LMWL equations used to calculate  $^{18}\text{O}_{\text{H}_2\text{O}}$  ‰ as follows: Daylesford  $\delta^2\text{H} = 7.5 \times \delta^{18}\text{O} + 9.8$  (Crosbie et al., 2012); Pah Tempe  $\delta^2\text{H} = 6.7 \times \delta^{18}\text{O} - 12.6$  (Kendall and Coplen, 2001).

Sample ID	Temperature °C	$\delta^2\text{H}$ ‰	$^{18}\text{O}_{\text{H}_2\text{O}}^i$ ‰	$\delta^{18}\text{O}_{\text{CO}_2}$ ‰	$^{18}\text{O}_{\text{H}_2\text{O}}^j$ ‰	$\epsilon_{\text{CO}_2-\text{H}_2\text{O}}$ ‰	$\Delta$ ‰	$\Delta - \epsilon$ ‰
<b>Pah Tempe springs, Utah, USA</b>								
S 7	40.6	−108.0	−13.0	26.3 ± 0.9	−14.2	37.2	39.0	1.8
S8	40.9	−108.3	−13.6	26.3 ± 0.9	−14.3	37.1	39.7	2.6
S 9	39.4	−107.7	−13.9	26.3 ± 0.9	−14.2	37.4	40.0	2.6
S 10	40	−108.7	−13.6	26.3 ± 0.9	−14.3	37.3	39.7	2.4
S 11	40	−108.5	−13.5	26.3 ± 0.9	−14.3	37.3	39.6	2.3
S 12	40.2 ± 0.6	−108.3	−13.2	26.3 ± 0.9	−14.3	37.2	39.2	2.0
S 13	40.2 ± 0.6	−108.4	−13.2	26.3 ± 0.9	−14.3	37.2	39.2	2.0
S 14	40.2 ± 0.6	−105.9	−12.8	26.3 ± 0.9	−13.9	37.2	38.8	1.6
S 15	40.2 ± 0.6	−108.3	−12.9	26.3 ± 0.9	−14.3	37.2	38.9	1.7
S 16	40.2 ± 0.6	−108.3	−12.8	26.3 ± 0.9	−14.3	37.2	38.8	1.6
S 17	40.2 ± 0.6	−108.6	−13.1	26.3 ± 0.9	−14.3	37.2	39.1	1.9
S 18	40.2 ± 0.6	−107.4	−13.7	26.3 ± 0.9	−14.1	37.2	39.8	2.6
S 19	40.2 ± 0.6	−108.9	−12.7	26.3 ± 0.9	−14.4	37.2	38.7	1.5
S 20	40.2 ± 0.6	−108.6	−13.0	26.3 ± 0.9	−14.3	37.2	39.0	1.8
S 21	40.2 ± 0.6	−108.2	−13.1	26.3 ± 0.9	−14.3	37.2	39.1	1.9
S 22	40.2 ± 0.6	−108.5	−13.6	26.3 ± 0.9	−14.3	37.2	39.7	2.5
S 23	40.2 ± 0.6	−108.4	−12.8	26.3 ± 0.9	−14.3	37.2	38.8	1.6
<b>Daylesford springs, SE Australia</b>								
Locarno spring-3	16.7	−34.58	−6.30	36.4	−5.4	41.9	42.1	0.2
Taradale spring-1	20.9	−33.10	−5.55	34.1	−5.2	41.0	39.1	−1.9

equilibrium with water enriched in  $^{18}\text{O}$  by up to 2‰ more than measured at the surface. Degassing in Daylesford is much more diffuse and episodic, allowing more time for equilibration with surface water, so partial equilibration has a less significant effect.

### 6.3.3. Kinetic fractionation on bubbles

An alternative or additional mechanism, which may deviate  $\delta^{18}\text{O}_{\text{CO}_2}$  from equilibrium, is kinetic fractionation during diffusion of dissolved species towards gas bubbles at the surface. Mass control on diffusivity leads to preferential uptake of  $^{12}\text{C}$  and  $^{16}\text{O}$  during bubble formation (Affek and Zaarur, 2014). If time is not sufficient for re-equilibration, the fractionation factor between  $\text{CO}_2$  and water will be lower than expected. In both localities gas samples were collected at the surface of bubbling streams and may therefore represent a lower-than-equilibrium  $\delta^{18}\text{O}_{\text{CO}_2}$  value.

Kinetic fractionation on bubbles has been extensively studied in relation to the volatile content in degassing volcanic melts (e.g. Aubaud et al., 2004; Paonita and Martelli, 2006). The effect has been observed as  $\delta^{13}\text{C}$  deviations of dissolved inorganic carbon (DIC) from equilibrium by up to 4‰ in groundwater springs, seepage waters and headwater catchments (Doctor et al., 2008), and up to 2.5‰ deviation from equilibrium in DIC  $\delta^{13}\text{C}$  samples collected at cold water springs in Green River, Utah (Assayag et al., 2009). The extent of kinetic fractionation increases with water pH and decreases with the depth of degassing. Liquids with lower volatile supersaturation are reported to show lower kinetic fractionation effects as equilibrium can be re-established quicker (Affek and Zaarur, 2014).

The limited availability of  $\delta^{18}\text{O}_{\text{CO}_2}$  measurements does not allow a quantitative comparison between the deviation from equilibrium in springs relative to measured pH and DIC contents. Generally, more actively degassing springs would be expected to deviate from equilibrium more, which agrees with field observations of higher gas discharge rates at Pah Tempe relative to Daylesford.

## 7. Summary

Water and  $\text{CO}_2$  sampled at the surface is unlikely to be in

equilibrium due to the secondary effects of localised partial equilibration and kinetic fractionation during gas ascent to the surface. Water salinity is unlikely to have an effect. Values of  $\delta^{18}\text{O}_{\text{CO}_2}$  from high flux springs in Pah Tempe and Taradale spring in Daylesford suggest that the oxygen isotope signature from localised equilibration at depth is preserved.  $\text{CO}_2$  from diffuse Daylesford springs (e.g. Locarno) re-equilibrates with dilute shallow water. The  $\delta^{18}\text{O}_{\text{CO}_2}$  values of gas collected at the water surface may be further obscured by  $^{18}\text{O}$  depletion during bubble formation, which affects high flux springs more than those with a diffuse low flux.

### 7.1. Implications for usage of $\delta^{18}\text{O}$ values in geothermometry

Water  $^{18}\text{O}$  enrichment relative to the MWL with no effect on  $\delta^2\text{H}$  has been traditionally associated with geothermal systems. Waters enriched in  $^{18}\text{O}$  are produced by isotopic exchange between hydrothermal fluids and bedrock minerals, normally at temperatures above 250 °C (Clark and Fritz, 1997; D'Amore and Panichi, 1987). The fractionation factor between any mineral and fluid is governed by temperature, thus allowing the distribution of isotopes to be used as a geothermometer (e.g. Giggenbach, 1992). Another mechanism is water–steam separation above liquid–vapour isotopic exchange at 220 °C. At this temperature oxygen is kinetically fractionated between fluid and vapour but there is no fractionation in hydrogen isotopes (Clark and Fritz, 1997). Due to the lack of other reported water  $^{18}\text{O}$  enriching mechanisms, it has become common practice to interpret  $^{18}\text{O}$  enrichment in reservoir water as evidence for geothermal conditions (e.g. Cerón et al., 1998; Nelson et al., 2009).

Here, we present evidence that oxygen isotope exchange with  $\text{CO}_2$  can result in  $^{18}\text{O}$ -enriched waters, if the starting  $\delta^{18}\text{O}$  value of  $\text{CO}_2$  is significantly higher than that of the water and if high gas to water ratios are present. The oxygen isotope exchange between  $\text{CO}_2$  and the spring waters provides a more robust explanation for the  $^{18}\text{O}$ -enriched waters from Pah Tempe springs, which is in closer agreement with the geothermometric calculations and water discharge temperatures without invoking circulation depths of over 5 km and equilibration at temperatures >150 °C as quoted in

Nelson et al. (2009).

Our findings have two significant implications. Firstly, CO<sub>2</sub>-water equilibration alone, without the need to invoke any additional processes, may result in water <sup>18</sup>O enrichment or depletion, which means that <sup>18</sup>O-enriched waters should not be solely interpreted as geothermal as is the current practice. Secondly, equilibrium achieved between water and minerals at depth may be obscured by later interaction with CO<sub>2</sub>. Both of these scenarios have significant implications to the sulfate-water oxygen isotope geothermometry technique, which relies on temperature and pH-dependant oxygen isotope exchange between water and dissolved SO<sub>4</sub>, applicable to temperature ranges between 140 and 350 °C (McKenzie and Truesdell, 1977). The method requires estimation of the water δ<sup>18</sup>O in equilibrium with sampled sulfate under an assumption that the original value has not been altered by secondary processes such as dilution with shallow water, boiling and steam loss, near-surface oxidation of H<sub>2</sub>S and biological activity or an application of an appropriate correction (Fowler et al., 2013). Equilibration with CO<sub>2</sub>, which can be achieved in a matter of hours and either deplete or enrich water in <sup>18</sup>O, should also be considered when using this geothermometry technique in CO<sub>2</sub>-rich waters. This consideration may also be significant to palaeowater studies which relate δ<sup>18</sup>O values of precipitating phases to either the palaeowater composition or precipitation temperatures (e.g. Astin and Scotchman, 1988; Morad and Eshete, 1990).

A recent study by Ladd and Ryan (2016) demonstrated that shallow surface build up in CO<sub>2</sub> partial pressure and subsequent bubble formation may be the main driving mechanism for geyser eruption in sub-boiling conditions, challenging the common notion that subsurface water boiling is required for this phenomena. Our study provides additional evidence that elevated CO<sub>2</sub> concentrations at ambient temperatures may explain the features often attributed to geothermal systems.

## 8. Conclusions

Global natural CO<sub>2</sub>-rich mineral waters show δ<sup>18</sup>O deviations from the MWL with no observed change in δ<sup>2</sup>H. Oxygen isotope deviations without a change in hydrogen isotopes may be the result of oxygen isotope equilibrium exchange between CO<sub>2</sub> and water, mineral dissolution and re-precipitation, or isotopic exchange with minerals. We have developed a simple geochemical modelling approach to study the influence of low temperature water-rock reactions on oxygen isotope changes in subsurface waters. The method requires knowledge of the water geochemistry (major ion concentrations, dissolved carbon content, pH, temperature) and a conceptual model of reactive and precipitating phases. Numerical modelling can be applied to assess the water-rock interaction influence on oxygen isotope ratios in other saline natural waters or CO<sub>2</sub> storage sites where oxygen isotopes are used as natural tracer of the injected CO<sub>2</sub> plume.

In two case studies from Daylesford (Australia) and Pah Tempe (Utah, USA), we apply our new modelling approach to show that low temperature water-rock reactions are unlikely to have a significant effect on water δ<sup>18</sup>O values. In both cases, the water δ<sup>18</sup>O shift can be explained by oxygen isotope exchange with CO<sub>2</sub>. Oxygen isotope values observed in the waters measured at Daylesford and Pah Tempe springs are close to equilibrium with δ<sup>18</sup>O of the erupting CO<sub>2</sub>. Deviation from ideal equilibrium is likely due to localised CO<sub>2</sub> movement through the water and the establishment of partial equilibration or kinetic isotope fractionation on degassing bubbles sampled at the water surface.

Traditionally, enrichment in <sup>18</sup>O in the reservoir waters relative to the MWL has been interpreted to be the result of geothermal activity, while <sup>18</sup>O depletion is proposed to be due to CO<sub>2</sub>-water

interaction at lower temperatures. Our global dataset of oxygen and hydrogen isotope measurements in waters from low temperature CO<sub>2</sub> springs and the case studies presented from the Daylesford and Pah Tempe CO<sub>2</sub> springs provide evidence that equilibration with CO<sub>2</sub> can result in both <sup>18</sup>O enrichment and depletion in spring waters and therefore geothermal conditions are not necessary to produce <sup>18</sup>O-enriched waters. This should be considered in future studies, and used to re-interpret data from previous studies using the water and mineral stable isotope composition to infer water circulation depths, temperatures and local tectonic settings.

## Acknowledgements

R. Karolytė acknowledges the support of an EPSRC PhD studentship in partnership with Badley Geoscience Ltd. The authors acknowledge the funding provided by CO2CRC (036610/1). S. Serno was funded by the UK Carbon Capture and Storage Research Centre (UKCCSRC) Call 2 grant, G. Johnson and S. Gilfillan were partially supported by both UKCCSRC and Scottish Carbon Capture and Storage (SCCS) (EP/K000446/1). Steve Nelson of Brigham Young University, Utah is thanked for introducing Gilfillan to the Pah Tempe springs and assisting with gas sample collection and background data. We thank Allan Chivas for his assistance in the field during collection of samples for the Daylesford springs and obtaining measurements of water samples. We extend our thanks to Ian Cartwright for sharing his extensive knowledge on Daylesford springs and Jen Roberts for helping out with the fieldwork in Daylesford. We thank Terry Donnelly, Adrian Boyce and Tony Fallick at SUERC for their assistance in obtaining stable isotope measurements of gas samples.

## Appendix A. Supplementary data

Supplementary data related to this chapter can be found at <http://dx.doi.org/10.1016/j.apgeochem.2017.06.012>.

## References

- Affek, H.P., Zaarur, S., 2014. Kinetic isotope effect in CO<sub>2</sub> degassing: insight from clumped and oxygen isotopes in laboratory precipitation experiments. *Geochim. Cosmochim. Acta* 143, 319–330. <http://dx.doi.org/10.1016/j.gca.2014.08.005>.
- Assayag, N., Bickle, M., Kampman, N., Becker, J., 2009. Carbon isotopic constraints on CO<sub>2</sub> degassing in cold-water Geysers, Green River, Utah. *Energy Procedia* 1, 2361–2366. <http://dx.doi.org/10.1016/j.egypro.2009.01.307>.
- Astin, T.R., Scotchman, I.C., 1988. The diagenetic history of some septarian concretions from the Kimmeridge Clay, England. *Sedimentology* 35, 349–368. <http://dx.doi.org/10.1111/j.1365-3091.1988.tb00952.x>.
- Aubaud, C., Pineau, F., Jambon, A., Javoy, M., 2004. Kinetic disequilibrium of C, He, Ar and carbon isotopes during degassing of mid-ocean ridge basalts. *Earth Planet. Sci. Lett.* <http://dx.doi.org/10.1016/j.epsl.2004.03.001>.
- Ball, J.W., Nordstrom, D.K., 1991. User's Manual for WATEQ4F, with Revised Thermodynamic Data Base and Text Cases for Calculating Speciation of Major, Trace, and Redox Elements in Natural Waters (Open-File Rep).
- Becker, V., Myrtilinen, A., Nightingale, M., Shevalier, M., Rock, L., Mayer, B., Barth, J.C., 2015. Stable carbon and oxygen equilibrium isotope fractionation of supercritical and subcritical CO<sub>2</sub> with DIC and H<sub>2</sub>O in saline reservoir fluids. *Int. J. Greenh. Gas. Control* 39, 215–224. <http://dx.doi.org/10.1016/j.ijggc.2015.05.020>.
- Biek, R., 2003. *Geologic Map of the Hurricane Quadrangle Washington County, Utah*. USGS.
- Bierlein, F.P., Foster, D.A., Mcknight, S., Arne, D.C., 1999. Timing of gold mineralisation in the Ballarat goldfields, central Victoria: constraints from 40Ar/39Ar results. *Aust. J. Earth Sci.* 46, 301–309. <http://dx.doi.org/10.1046/j.1440-0952.1999.00708.x>.
- Bindeman, I., 2008. Oxygen isotopes in mantle and crustal magmas as revealed by single crystal analysis. *Rev. Mineral. Geochem.* 69, 445–478. <http://dx.doi.org/10.2138/rmg.2008.69.12>.
- Blomqvist, R.G., 1990. Deep groundwaters in the crystalline basement of Finland, with implications for nuclear waste disposal studies. *Geol. Foereningen i Stock. Foerhandlingar* 112, 369–374. <http://dx.doi.org/10.1080/11035899009452737>.
- Bottlinga, Y., 1968. Calculation of fractionation factors for carbon and oxygen isotopic exchange in the system calcite-carbon dioxide-water. *J. Phys. Chem.* 72, 800–808 doi:10.1021/j100849a008.

- Boyce, J., 2013. The Newer Volcanics Province of southeastern Australia: a new classification scheme and distribution map for eruption centres. *Aust. J. Earth Sci.* 60, 449–462. <http://dx.doi.org/10.1080/08120099.2013.806954>.
- Budding, K.E., Sommer, S.N., 1986. Low-temperature geothermal assessment of the Santa Clara and Virgin River valleys, Washington county, Utah. *Utah Geol. Miner. Surv.* 67, 34.
- Burden, C.B., 2015. Groundwater Conditions in Utah. Spring of 2015. Cooperative investigations report no. 56.
- Burns, S.J., Matter, A., 1995. Geochemistry of carbonate cements in surficial alluvial conglomerates and their paleoclimatic implications, sultanate of Oman. *J. Sediment. Res.* 65A, 170–177. <http://dx.doi.org/10.1306/D426805E-2B26-11D7-8648000102C1865D>.
- Cartwright, I., Weaver, T., Tweed, S., Ahearne, D., Cooper, M., Czapnik, C., Tranter, J., 2000. O, H, C isotope geochemistry of carbonated mineral springs in central Victoria, Australia: sources of gas and water-rock interaction during dying basaltic volcanism. *J. Geochem. Explor.* 69–70, 257–261. [http://dx.doi.org/10.1016/S0375-6742\(00\)00059-5](http://dx.doi.org/10.1016/S0375-6742(00)00059-5).
- Cartwright, I., Weaver, T., Tweed, S., Ahearne, D., Cooper, M., Czapnik, K., Tranter, J., 2002. Stable isotope geochemistry of cold CO<sub>2</sub>-bearing mineral spring waters, Daylesford, Victoria, Australia: sources of gas and water and links with waning volcanism. *Chem. Geol.* 185, 71–91. [http://dx.doi.org/10.1016/S0009-2541\(01\)00397-7](http://dx.doi.org/10.1016/S0009-2541(01)00397-7).
- Casanova, J., Bodéan, F., Négrel, P., Azaroual, M., 1999. Microbial control on the precipitation of modern ferrihydrite and carbonate deposits from the Cezallier hydrothermal springs (Massif Central, France). *Sediment. Geol.* 126, 125–145. [http://dx.doi.org/10.1016/S0037-0738\(99\)00036-6](http://dx.doi.org/10.1016/S0037-0738(99)00036-6).
- Cerón, J.C., Pulido-Bosch, A., 1999. Geochemistry of thermomineral waters in the overexploited Alto Guadalelín aquifer (south-east Spain). *Water Res.* 33, 295–300. [http://dx.doi.org/10.1016/S0043-1354\(98\)00175-4](http://dx.doi.org/10.1016/S0043-1354(98)00175-4).
- Cerón, J.C., Pulido-Bosch, A., Sanz De Galdeano, C., 1998. Isotopic identification of CO<sub>2</sub> from a deep origin in thermomineral waters of southeastern Spain. *Chem. Geol.* 149, 251–258. [http://dx.doi.org/10.1016/S0009-2541\(98\)00045-X](http://dx.doi.org/10.1016/S0009-2541(98)00045-X).
- Chivas, A.R., Barnes, I.E., Lupton, J.E., Collerson, K., 1983. Isotopic studies of south-east Australian CO<sub>2</sub> discharges. *Geol. Soc. Aust. Abstr.* 12, 94–95.
- Chivas, A.R., Barnes, I., Evans, W.C., Lupton, J.E., Stone, J.O., 1987. Liquid carbon dioxide of magmatic origin and its role in volcanic eruptions. *Nature* 326, 587–589. <http://dx.doi.org/10.1038/326587a0>.
- Cinti, D., Procesi, M., Tassi, F., Montegrossi, G., Sciarra, A., Vaselli, O., Quattrocchi, F., 2011. Fluid geochemistry and geothermometry, of the western sector of the Sabatini volcanic district and the Tolfa Mountains (Central Italy). *Chem. Geol.* 284, 160–181. <http://dx.doi.org/10.1016/j.chemgeo.2011.02.017>.
- Clark, I.D., Fritz, P., 1997. *Environmental Isotopes in Hydrogeology*. CRC Press/Lewis Publishers, Boca Raton, FL.
- Clayton, R.N., Steiner, A., 1975. Oxygen isotope studies of the geothermal system at Wairakei, New Zealand. *Geochim. Cosmochim. Acta* 39, 1179–1186. [http://dx.doi.org/10.1016/0016-7037\(75\)90059-9](http://dx.doi.org/10.1016/0016-7037(75)90059-9).
- Compton, J.S., Conrad, M.E., Vennemann, T.W., 1999. Stable isotope evolution of volcanic ash layers during diagenesis of the Miocene Monterey Formation, California. *Clays Clay Miner.* 47, 84–95. <http://dx.doi.org/10.1346/CCMN.1999.0470109>.
- Craig, H., 1961. Isotopic variations in meteoric waters. *Science* 133 (80), 1702–1703.
- Crosbie, R., Morrow, D., Cresswell, R., Leaney, F., Lamontagne, S., Lefournour, M., 2012. New Insights to the Chemical and Isotopic Composition of Rainfall across Australia, 86.
- Dansgaard, W., 1964. Stable isotopes in precipitation. *Tellus* 16, 436–468. <http://dx.doi.org/10.1111/j.2153-3490.1964.tb00181.x>.
- Delalande, M., Bergonzini, L., Gherardi, F., Guidi, M., Andre, L., Abdallah, I., Williamson, D., 2011. Fluid geochemistry of natural manifestations from the Southern Poroto-Rungwe hydrothermal system (Tanzania): preliminary conceptual model. *J. Volcanol. Geotherm. Res.* 199, 127–141. <http://dx.doi.org/10.1016/j.jvolgeores.2010.11.002>.
- Demlie, M., Titus, R., 2015. Hydrogeological and hydrogeochemical characteristics of the natal group sandstone, South Africa. *South Afr. J. Geol.* 118, 33–44. <http://dx.doi.org/10.2113/gssaj.118.1.33>.
- Doctor, D.H., Kendall, C., Sebestyen, S.D., Shanley, J.B., Ohte, N., Boyer, E.W., 2008. Carbon isotope fractionation of dissolved inorganic carbon (DIC) due to outgassing of carbon dioxide from a headwater stream. *Hydrol. Process* 22, 2410–2423. <http://dx.doi.org/10.1002/hyp.6833>.
- Dutson, S.J., 2005. Effects of Hurricane Fault Architecture on Groundwater Flow in the Timpoweap Canyon of Southwestern, Utah 57. MSc thesis. Brigham Young University. <http://scholarsarchive.byu.edu/etd/583/> (Accessed 9 December 2016).
- D'Amore, F., Panichi, C., 1987. Geochemistry in geothermal exploration. *Appl. Geotherm.* 9, 69–89.
- Fowler, A.P.G., Hackett, L.B., Klein, C.W., 2013. Reformulation and performance evaluation of the sulfate-water oxygen isotope geothermometer. In: *GRC Transactions*, p. 31. GRC Annual Meeting.
- Frape, S.K., Fritz, P., 1982. The chemistry and isotopic composition of saline groundwaters from the Sudbury Basin, Ontario. *Can. J. Earth Sci.* 19, 645–661. <http://dx.doi.org/10.1139/e82-053>.
- Friedman, I., O'Neil, J.R., 1977. Compilation of stable isotope fractionation factors of geochemical interest [Data of Geochemistry, sixth edition]. U. S. Geol. Surv. Prof. Pap. 440, 12. [http://dx.doi.org/10.1016/S0016-0032\(20\)90415-5](http://dx.doi.org/10.1016/S0016-0032(20)90415-5).
- Giggenbach, W.F., 1992. Isotopic shifts in waters from geothermal and volcanic systems along convergent plate boundaries and their origin. *Earth Planet. Sci. Lett.* 113, 495–510. [http://dx.doi.org/10.1016/0012-821X\(92\)90127-H](http://dx.doi.org/10.1016/0012-821X(92)90127-H).
- Harris, C., Stock, W.D., Lanham, J., 1997. Stable isotope constraints on the origin of CO<sub>2</sub> gas exhalations at Bongwan, Natal. *South Afr. J. Geol.* 100, 261–266.
- Hays, P.D., Grossman, E.L., 1991. Oxygen isotopes in meteoric calcite cements as indicators of continental paleoclimate. *Geology*. [http://dx.doi.org/10.1130/0091-7613\(1991\)019<0441:OIMCC>2.3.CO;2](http://dx.doi.org/10.1130/0091-7613(1991)019<0441:OIMCC>2.3.CO;2).
- Hearn, P.P., Steinkampf, W.C., Horton, D.G., Solomon, G.C., White, L.D., Evans, J.R., 1989. Oxygen-isotope composition of ground water and secondary minerals in Columbia Plateau basalts: implications for the paleohydrology of the Pasco Basin. *Geology*. [http://dx.doi.org/10.1130/0091-7613\(1989\)017<0606:OICOGW>2.3.CO;2](http://dx.doi.org/10.1130/0091-7613(1989)017<0606:OICOGW>2.3.CO;2).
- Humez, P., Lions, J., Négrel, P., Lagneau, V., 2014. CO<sub>2</sub> intrusion in freshwater aquifers: review of geochemical tracers and monitoring tools, classical uses and innovative approaches. *Appl. Geochem.* 46, 95–108. <http://dx.doi.org/10.1016/j.apgeochem.2014.02.008>.
- Johnson, G., Mayer, B., 2011. Oxygen isotope exchange between H<sub>2</sub>O and CO<sub>2</sub> at elevated CO<sub>2</sub> pressures: implications for monitoring of geological CO<sub>2</sub> storage. *Appl. Geochem.* 26, 1184–1191. <http://dx.doi.org/10.1016/j.apgeochem.2011.04.007>.
- Johnson, G., Mayer, B., Nightingale, M., Shevalier, M., Hutcheon, I., 2011. Using oxygen isotope ratios to quantitatively assess trapping mechanisms during CO<sub>2</sub> injection into geological reservoirs: the Pembina case study. *Chem. Geol.* 283, 185–193. <http://dx.doi.org/10.1016/j.chemgeo.2011.01.016>.
- Kampman, N., Bickle, M., Wigley, M., Dubacq, B., 2014. Fluid flow and CO<sub>2</sub>-fluid-mineral interactions during CO<sub>2</sub>-storage in sedimentary basins. *Chem. Geol.* 369, 22–50. <http://dx.doi.org/10.1016/j.chemgeo.2013.11.012>.
- Kendall, C., Coplen, T.B., 2001. Distribution of oxygen-18 and deuterium in river waters across the United States. *Hydrol. Process* 15, 1363–1393. <http://dx.doi.org/10.1002/hyp.217>.
- Kharaka, Y.K., Cole, D.R., Hovorka, S.D., Gunter, W.D., Knauss, K.G., Freifeld, B.M., 2006. Gas-water-rock interactions in Frio Formation following CO<sub>2</sub> injection: implications for the storage of greenhouse gases in sedimentary basins. *Geology* 34, 577–580. <http://dx.doi.org/10.1130/G22357.1>.
- Kloppmann, W., Girard, J.P., Négrel, P., 2002. Exotic stable isotope compositions of saline waters and brines from the crystalline basement. *Chem. Geol.* 184, 49–70. [http://dx.doi.org/10.1016/S0009-2541\(01\)00352-7](http://dx.doi.org/10.1016/S0009-2541(01)00352-7).
- Kristmannsdóttir, H., Sveinbjörnsdóttir, A.E., 2012. An anomalous thermal water from Hofstadir western Iceland: evidence for past CO<sub>2</sub> flushing. *Appl. Geochem.* 27, 1146–1152. <http://dx.doi.org/10.1016/j.apgeochem.2012.02.030>.
- Ladd, B.S., Ryan, M.C., 2016. Can CO<sub>2</sub> trigger a thermal geyser eruption? *Geology* 44, 307–310. <http://dx.doi.org/10.1130/G37588.1>.
- Lawrence, C.R., 1969. Hydrogeology of the Daylesford Mineral District with special reference to the mineral springs. *Geol. Surv. Vic. Undergr. Water Investig. Rep.* 12.
- Lécuyer, C., Gardien, V., Rigaudier, T., Fourel, F., Martineau, F., Cros, A., 2009. Oxygen isotope fractionation and equilibration kinetics between CO<sub>2</sub> and H<sub>2</sub>O as a function of salinity of aqueous solutions. *Chem. Geol.* 264, 122–126. <http://dx.doi.org/10.1016/j.chemgeo.2009.02.017>.
- Lions, J., Humez, P., Pauwels, H., Kloppmann, W., Czernichowski-Lauriol, I., 2014. Tracking leakage from a natural CO<sub>2</sub> reservoir (Montmirail, France) through the chemistry and isotope signatures of shallow groundwater. *Greenh. Gases Sci. Technol.* 4, 225–243. <http://dx.doi.org/10.1002/ghg.1381>.
- Losh, S., Eglington, L., Schoell, M., Wood, J., 1999. Vertical and lateral fluid flow related to a large growth fault, South Eugene Island Block 330 field, offshore Louisiana. *Am. Assoc. Pet. Geol. Bull.* 83, 244–276. <http://dx.doi.org/10.1306/00AA9A5C-1730-11D7-8645000102C1865D>.
- Marques, J.M., Carreira, P.M.M., Aires-Barros, L., Graça, R.C., 2000. Nature and role of CO<sub>2</sub> in some hot and cold HCO<sub>3</sub><sup>-</sup>/Na<sup>+</sup>/CO<sub>2</sub>-rich Portuguese mineral waters: a review and reinterpretation. *Environ. Geol.* 40, 53–63. <http://dx.doi.org/10.1007/s002540000151>.
- Matsuhisa, Y., Goldsmith, J.R., Clayton, R.N., 1979. Oxygen isotopic fractionation in the system quartz-albite-anorthite-water. *Geochim. Cosmochim. Acta* 43, 1131–1140. [http://dx.doi.org/10.1016/0016-7037\(79\)90099-1](http://dx.doi.org/10.1016/0016-7037(79)90099-1).
- Matthews, A., Palin, J., Epstein, S., Stolper, E., 1994. Experimental study of partitioning between crystalline albite, albitic glass and CO<sub>2</sub> gas. *Geochim. Cosmochim. Acta* 58, 5255–5266. [http://dx.doi.org/10.1016/0016-7037\(94\)90309-3](http://dx.doi.org/10.1016/0016-7037(94)90309-3).
- May, F., 2005. Alteration of wall rocks by CO<sub>2</sub>-rich water ascending in fault zones: natural analogues for reactions induced by CO<sub>2</sub> migrating along faults in siliclastic reservoir and cap rocks. *Oil Gas. Sci. Technol.* 60, 19–32. <http://dx.doi.org/10.2516/ogst.2005003>.
- McKenzie, W.F., Truesdell, A.H., 1977. Geothermal reservoir temperatures estimated from the oxygen isotope compositions of dissolved sulfate and water from hot springs and shallow drillholes. *Geothermics* 5, 51–61. [http://dx.doi.org/10.1016/0375-6505\(77\)90008-6](http://dx.doi.org/10.1016/0375-6505(77)90008-6).
- Morad, S., Eshete, M., 1990. Petrology, chemistry and diagenesis of calcite concretions in Silurian shales from central Sweden. *Sediment. Geol.* 66, 113–134. [http://dx.doi.org/10.1016/0037-0738\(90\)90010-Q](http://dx.doi.org/10.1016/0037-0738(90)90010-Q).
- Nelson, S.T., Mayo, A.L., Gillfillan, S., Dutson, S.J., Harris, R.A., Shipton, Z.K., Tingey, D.G., 2009. Enhanced fracture permeability and accompanying fluid flow in the footwall of a normal fault: the Hurricane fault at Pah Tempe hot springs, Washington County, Utah. *Geol. Soc. Am. Bull.* <http://dx.doi.org/10.1130/B26285.1> preprint, 1.
- Paonita, A., Martelli, M., 2006. Magma dynamics at mid-ocean ridges by noble gas kinetic fractionation: assessment of magmatic ascent rates. *Earth Planet. Sci. Lett.* <http://dx.doi.org/10.1016/j.epsl.2005.10.018>.

- Parkhurst, D.L., Appelo, C.A.J., 1999. User's Guide to PHREEQC (Version 2): a Computer Program for Speciation, Batch-reaction, One-dimensional Transport, and Inverse Geochemical Calculations.
- Pauwels, H., Fouillac, C., Goff, F., Vuataz, F.D., 1997. The isotopic and chemical composition of CO<sub>2</sub>-rich thermal waters in the Mont-Dore region (Massif-Central, France). *Appl. Geochem.* 12, 411–427. [http://dx.doi.org/10.1016/S0883-2927\(97\)00010-3](http://dx.doi.org/10.1016/S0883-2927(97)00010-3).
- Pauwels, H., Gaus, I., le Nindre, Y.M., Pearce, J., Czernichowski-Lauriol, I., 2007. Chemistry of fluids from a natural analogue for a geological CO<sub>2</sub> storage site (Montmiral, France): lessons for CO<sub>2</sub>-water-rock interaction assessment and monitoring. *Appl. Geochem.* 22, 2817–2833. <http://dx.doi.org/10.1016/j.apgeochem.2007.06.020>.
- Plampin, M.R., Lassen, R.N., Sakaki, T., Porter, M.L., Pawar, R.J., Jensen, K.H., Illangasekare, T.H., 2014. Heterogeneity-enhanced gas phase formation in shallow aquifers during leakage of CO<sub>2</sub>-saturated water from geologic sequestration sites. *Water Resour. Res.* 50, 9251–9266. <http://dx.doi.org/10.1002/2014WR015715>.
- Price, R.C., Nicholls, L.A., Gray, C.M., 2003. Cainozoic igneous activity. In: Birch, W.D. (Ed.), *Geology of Victoria*. Geological Society of Australia (Victoria Division), pp. 361–375. Special publication 23.
- Richet, P., Bottinga, Y., Javoy, M., 1977. A review of hydrogen, carbon, nitrogen, oxygen, sulphur, and chlorine stable isotope fractionation among gaseous molecules. *Annu. Rev. Earth Planet. Sci.* 5, 65–110. <http://dx.doi.org/10.1146/annurev.ea.05.050177.000433>.
- Roberts, J.J., Wood, R.A., Wilkinson, M., Haszeldine, S., 2015. Surface controls on the characteristics of natural CO<sub>2</sub> seeps: implications for engineered CO<sub>2</sub> stores. *Geofluids* 15, 453–463. <http://dx.doi.org/10.1111/gfl.12121>.
- Rozanski, K., Araguás-Araguás, L., Gonfiantini, R., 1993. Isotopic patterns in modern global precipitation. *Clim. Chang. Cont. Isot. Rec.* 78, 1–36. <http://dx.doi.org/10.1029/GM078p0001>.
- Serno, S., Johnson, G., LaForce, T.C., Ennis-King, J., Haese, R.R., Boreham, C.J., Paterson, L., Freifeld, B.M., Cook, P.J., Kirste, D., Haszeldine, R.S., Gilfillan, S.M.V., 2016. Using oxygen isotopes to quantitatively assess residual CO<sub>2</sub> saturation during the CO<sub>2</sub>CRC Otway Stage 2B Extension residual saturation test. *Int. J. Greenh. Gas. Control* 52, 73–83. <http://dx.doi.org/10.1016/j.ijggc.2016.06.019>.
- Sheppard, S.M.F., Gilg, H.A., 1996. Stable isotope geochemistry of clay minerals. *Clay Miner* 31, 1–24.
- Shugg, A., 2009. Hepburn spa: cold carbonated mineral waters of central Victoria, south eastern Australia. *Environ. Geol.* 58, 1663–1673. <http://dx.doi.org/10.1007/s00254-008-1610-8>.
- Siegel, D.I., Lesniak, K. a., Stute, M., Frapre, S., 2004. Isotopic geochemistry of the Saratoga springs: implications for the origin of solutes and source of carbon dioxide. *Geology* 32, 257–260. <http://dx.doi.org/10.1130/G20094.1>.
- Sterpenich, J., Sausse, J., Pironon, J., Géhin, A., Hubert, G., Perfetti, E., Grgic, D., 2009. Experimental ageing of oolitic limestones under CO<sub>2</sub> storage conditions. *Chem. Geol.* 265, 99–112. <http://dx.doi.org/10.1016/j.chemgeo.2009.04.011>.
- Thomas, D.L., Bird, D.K., Arnórsson, S., Maher, K., 2016. Geochemistry of CO<sub>2</sub>-rich waters in Iceland. *Chem. Geol.* 444, 158–179. <http://dx.doi.org/10.1016/j.chemgeo.2016.09.002>.
- Truesdell, A.H., 1974. Oxygen isotope activities and concentrations in aqueous salt solutions at elevated temperatures: consequences for isotope geochemistry. *Earth Planet. Sci. Lett.* 23, 387–396. [http://dx.doi.org/10.1016/0012-821X\(74\)90128-9](http://dx.doi.org/10.1016/0012-821X(74)90128-9).
- Vuataz, F.D., Goff, F., 1986. Isotope geochemistry of thermal and nonthermal waters in the Valles Caldera, Jemez Mountains, northern New Mexico. *J. Geophys. Res.* 91, 1835–1853. <http://dx.doi.org/10.1029/JB091iB02p01835>.
- Watson, M.N., Boreham, C.J., Tingate, P.R., 2004. Carbon Dioxide and Carbonate Cements in the Otway Basin; Implications for Geological Storage of Carbon Dioxide, 2004 APPEA conference. 2004 APPEA Conf. Canberra, Aust. March 28–31, 2004 44, no.1.
- Weaver, T.R., Cartwright, I., Tweed, S.O., Ahearne, D., Cooper, M., Czapnik, K., Tranter, J., 2006. Controls on chemistry during fracture-hosted flow of cold CO<sub>2</sub>-bearing mineral waters, Daylesford, Victoria, Australia: implications for resource protection. *Appl. Geochem.* 21, 289–304. <http://dx.doi.org/10.1016/j.apgeochem.2005.09.011>.
- Wilkinson, M., Gilfillan, S.M.V., Haszeldine, R.S., Ballentine, C.J., 2009. Plumbing the depths: testing natural tracers of subsurface CO<sub>2</sub> origin and migration, Utah, in: carbon dioxide sequestration in geological media-state of the science. *AAPG Spec. Vol.* 619–634. <http://dx.doi.org/10.1306/13171266St591353>.
- Young, E.D., Galy, A., Nagahara, H., 2002. Kinetic and equilibrium mass-dependant isotope fractionation laws in nature and their geochemical and cosmochemical significance. *Geochim. Cosmochim. Acta* 66, 1095–1104. [http://dx.doi.org/10.1016/S0016-7037\(01\)00832-8](http://dx.doi.org/10.1016/S0016-7037(01)00832-8).
- Zhao, Z.-F., Zheng, Y.-F., 2003. Calculation of oxygen isotope fractionation in magmatic rocks. *Chem. Geol.* 193, 59–80. [http://dx.doi.org/10.1016/S0009-2541\(02\)00226-7](http://dx.doi.org/10.1016/S0009-2541(02)00226-7).
- Zheng, Y.-F., 1999. Oxygen isotope fractionation in carbonate and sulfate minerals. *Geochem. J.* 33, 109–126. <http://dx.doi.org/10.2343/geochemj.33.109>.
- Zheng, Y.F., 2011. On the theoretical calculations of oxygen isotope fractionation factors for carbonate-water systems. *Geochem. J.* 45, 341–354. <http://dx.doi.org/10.2343/geochemj.1.0125>.
- Ziegler, K., 2006. Clay minerals of the permian rotliegend group in the north sea and adjacent areas. *Clay Miner* 41, 355–393. <http://dx.doi.org/10.1180/0009855064110200>.